INFN-ISRO Contract No. LEAO 2011 000 261 0101FE

Thermo-optical vacuum testing of IRNSS LRA qualification model

L. Porcelli*†, S. Dell'Agnello†, R. Venkateswaran‡, P. Chakraborty‡, C. V. Ramana Reddy‡, K. V. Sriram‡, A. Boni†, C. Cantone†, E. Ciocci†, S. Contessa†, G. Delle Monache†, N. Intaglietta†, L. Salvatori†, C. Lops†, M. Martini†, G. Patrizi†, M. Tibuzzi†, C. Mondaini†, P. Tuscano†, M. Maiello†

† Istituto Nazionale di Fisica Nucleare - Laboratori Nazionali di Frascati, Via E. Fermi 40, 00044 Frascati, Rome, Italy.

‡ Indian Space Research Organisation - Laboratory for Electro-Optics Systems, First Cross, First Phase, Peenya Industrial Estate, Bangalore - 560 058, India.

* Corresponding author: luca.porcelli@lnf.infn.it

Introduction

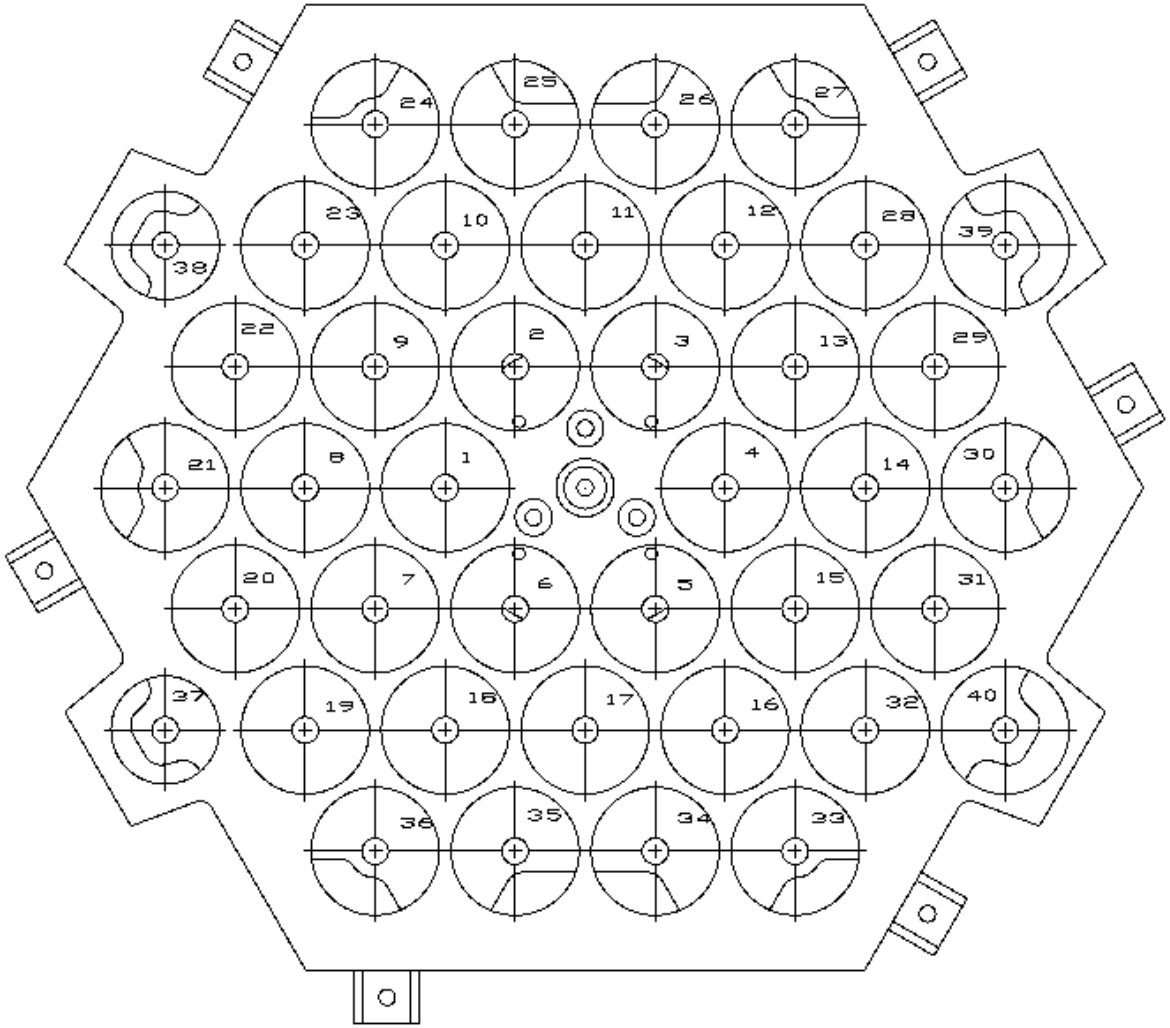

Introduction

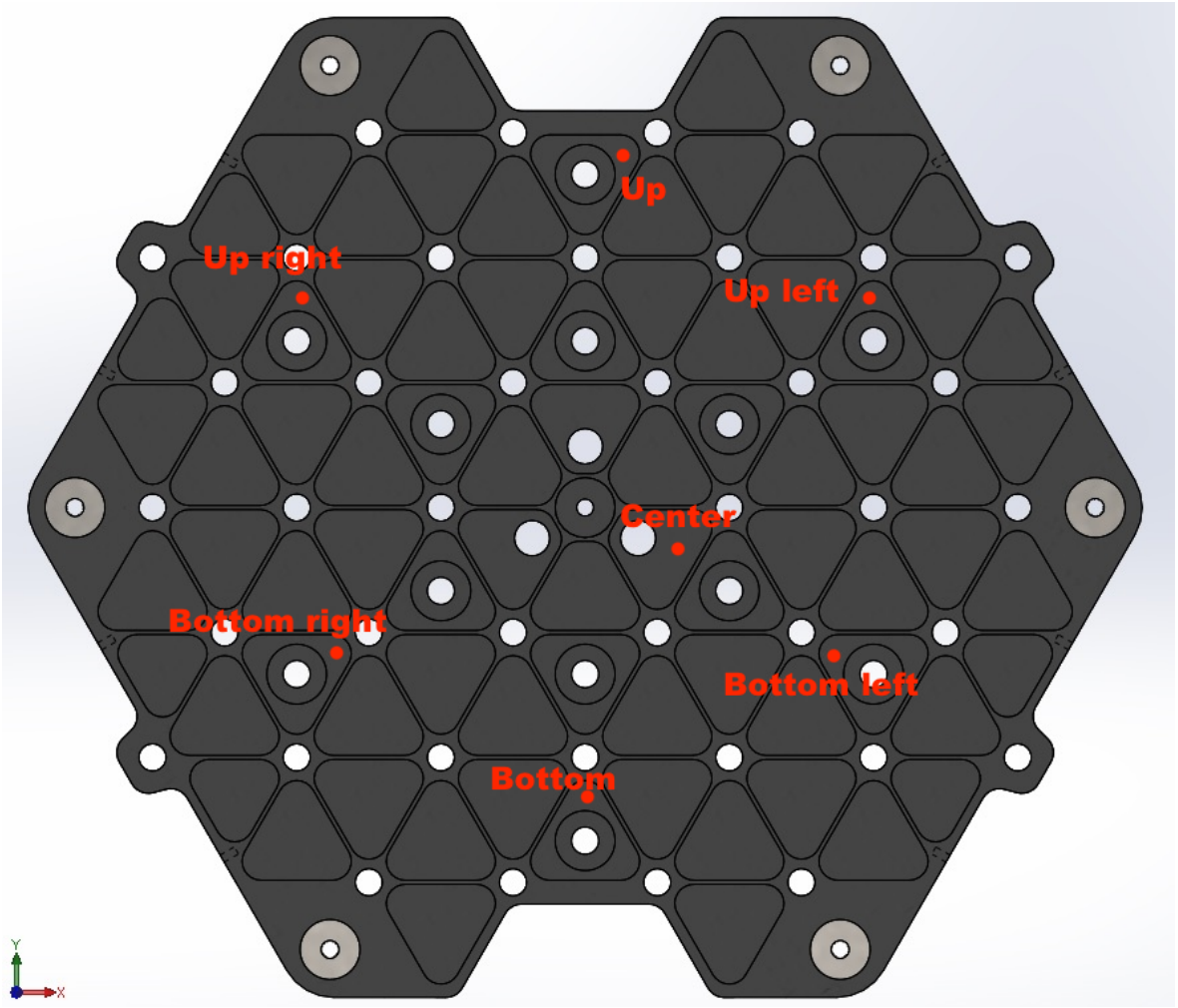

LRA in-air and isothermal FFDP measurements

Test structure:

- Measurements in Air and isothermal condition of all the CCRRs of the IRNSS LRA.
- Three different inclination angles: with array in front of the laser window, namely 0 degrees, and ±9 degrees laser incidence (positive = clockwise rotation as seen from above).
- We acquire the CCRR energy distribution of both the polarization components, horizontal and vertical.

Analysis:

- Analysis of raw optical measured data with a dedicated MATLAB program.
- For each tested CCRR and laser incidence angle the program computes:
  - The Field Diffraction Pattern (FFDP) in Optical Cross Section (OCS) unit.
  - OCS intensity distribution versus velocity aberration.
  - OCS intensity distribution in annulus at 18 µrad velocity aberration.
  - Average OCS intensity at 18 µrad velocity aberration a total CCRR FFDP.

LRA in-air and isothermal FFDP measurements

0° Laser incidence

FFDP and the intensity versus VA

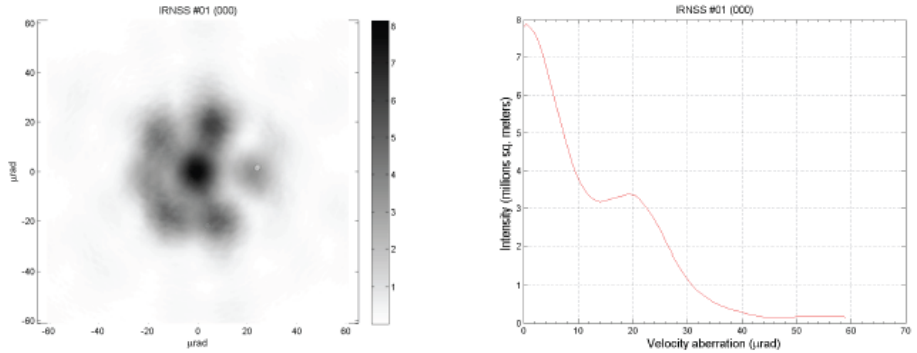

Figure 2:Left: FFDP; right: average intensity versus velocity aberration of CCRR n.01.

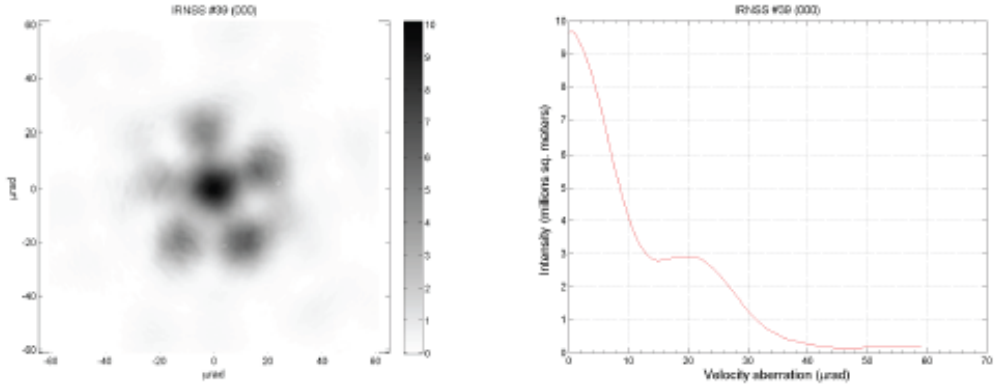

Figure 40: Left: FFDP; right: average intensity versus velocity aberration of CCRR n.39.

Table 1: Measured data of central peak intensity of every CCRRs.

ccrr_num	orientation	X [mm]	Y [mm]	Central Peak Intensity [m^2]
irn_01	0°	0.0	0.0	3.83E+06
irn_02	0°	26.5	45.9	7.66E+06
irn_03	0°	79.5	45.9	7.86E+06
irn_04	0°	106.0	0.0	4.27E+06
irn_05	0°	79.5	-45.9	5.81E+06
irn_06	0°	26.5	-45.9	5.68E+06
irn_07	0°	-26.5	-45.9	6.60E+06
irn_08	0°	-53.0	0.0	6.91E+06
irn_09	0°	-26.5	45.9	6.02E+06
irn_10	0°	0.0	91.8	6.94E+06
irn_11	0°	53.0	91.8	8.20E+06
irn_12	0°	106.0	91.8	6.87E+06
irn_13	0°	132.5	45.9	6.41E+06
irn_14	0°	159.0	0.0	6.93E+06
irn_15	0°	132.5	-45.9	8.62E+06
irn_16	0°	106.0	-91.8	7.12E+06
irn_17	0°	53.0	-91.8	7.51E+06
irn_18	0°	0.0	-91.8	7.76E+06
irn_19	0°	-53.0	-91.8	6.72E+06
irn_20	0°	-79.5	-45.9	6.49E+06
irn_21	0°	-106.0	0.0	5.78E+06
irn_22	0°	-79.5	45.9	6.40E+06
irn_23	0°	-53.0	91.8	7.25E+06
irn_24	0°	-26.5	137.7	7.06E+06
irn_25	0°	26.5	137.7	6.08E+06
irn_26	0°	79.5	137.7	7.88E+06
irn_27	0°	132.5	137.7	5.91E+06
irn_28	0°	159.0	91.8	6.64E+06
irn_29	0°	185.5	45.9	7.80E+06
irn_30	0°	212.0	0.0	4.76E+06
irn_31	0°	185.5	-45.9	5.53E+06
irn_32	0°	159.0	-91.8	4.39E+06
irn_33	0°	132.5	-137.7	7.06E+06
irn_34	0°	79.5	-137.7	5.31E+06
irn_35	0°	26.5	-137.7	3.34E+06
irn_36	0°	-26.5	-137.7	5.66E+06
irn_37	0°	-106.0	-91.8	4.88E+06
irn_38	0°	-106.0	91.8	6.81E+06
irn_39	0°	212.0	91.8	5.79E+06
irn_40	0°	212.0	-91.8	7.07E+06

LRA in-air and isothermal FFDP measurements

+9° Laser incidence

FFDP and the intensity versus VA

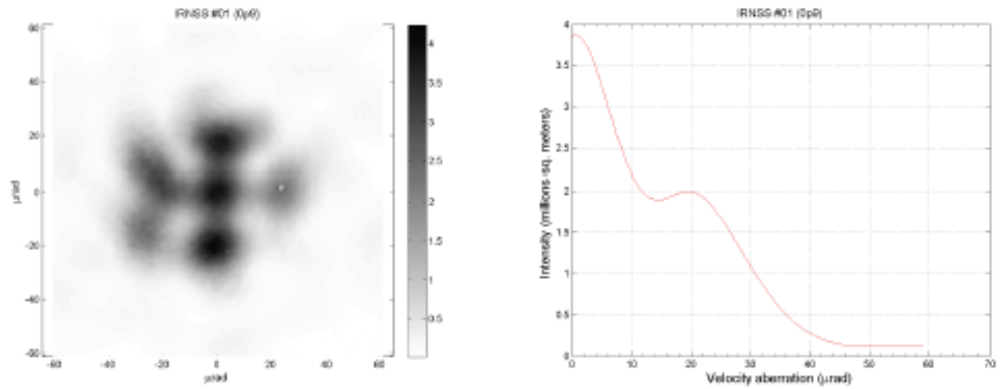

Figure 42: Left: FFDP; right: average intensity versus velocity aberration of CCRR n.01.

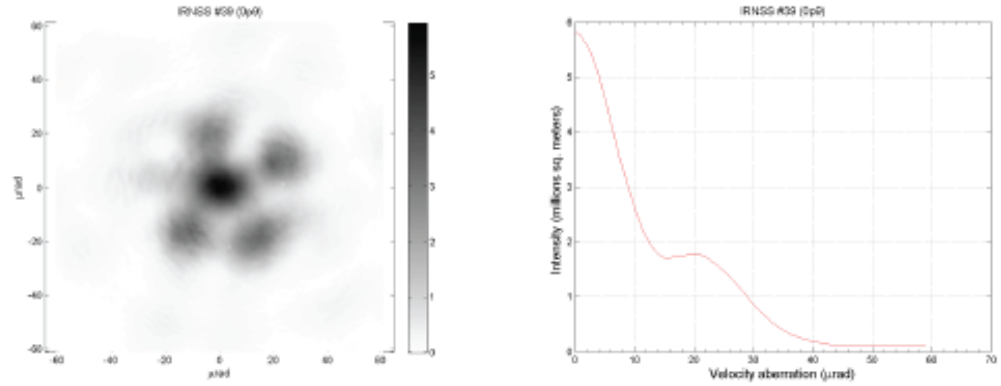

Figure 80: Left: FFDP; right: average intensity versus velocity aberration of CCRR n.39.

Table 2: Measured data of central peak intensity of every CCRRs.

ccrr_num	orientation	X [mm]	Y [mm]	Central Peak Intensity [m^2]
irn_01	+9°	0.0	0.0	3.83E+06
irn_02	+9°	26.2	45.9	7.66E+06
irn_03	+9°	78.5	45.9	7.86E+06
irn_04	+9°	104.7	0.0	4.27E+06
irn_05	+9°	78.5	-45.9	5.81E+06
irn_06	+9°	26.2	-45.9	5.68E+06
irn_07	+9°	-26.1	-45.9	6.60E+06
irn_08	+9°	-52.3	0.0	6.91E+06
irn_09	+9°	-26.1	45.9	6.02E+06
irn_10	+9°	0.0	91.8	6.94E+06
irn_11	+9°	52.4	91.8	8.20E+06
irn_12	+9°	104.7	91.8	6.87E+06
irn_13	+9°	130.9	45.9	6.41E+06
irn_14	+9°	157.1	0.0	6.93E+06
irn_15	+9°	130.9	-45.9	8.62E+06
irn_16	+9°	104.7	-91.8	7.12E+06
irn_17	+9°	52.4	-91.8	7.51E+06
irn_18	+9°	0.0	-91.8	7.76E+06
irn_19	+9°	-52.3	-91.8	6.72E+06
irn_20	+9°	-78.5	-45.9	6.49E+06
irn_21	+9°	-104.7	0.0	5.78E+06
irn_22	+9°	-78.5	45.9	6.40E+06
irn_23	+9°	-52.3	91.8	7.25E+06
irn_24	+9°	-26.1	137.7	7.06E+06
irn_25	+9°	26.2	137.7	6.08E+06
irn_26	+9°	78.5	137.7	7.88E+06
irn_27	+9°	130.9	137.7	5.91E+06
irn_28	+9°	157.1	91.8	6.64E+06
irn_29	+9°	183.2	45.9	7.80E+06
irn_30	+9°	209.4	0.0	4.76E+06
irn_31	+9°	183.2	-45.9	5.53E+06
irn_32	+9°	157.1	-91.8	4.39E+06
irn_33	+9°	130.9	-137.7	7.06E+06
irn_34	+9°	78.5	-137.7	5.31E+06
irn_35	+9°	26.2	-137.7	3.34E+06
irn_36	+9°	-26.1	-137.7	5.66E+06
irn_37	+9°	-104.7	-91.8	4.88E+06
irn_38	+9°	-104.7	91.8	6.81E+06
irn_39	+9°	209.4	91.8	5.79E+06
irn_40	+9°	209.4	-91.8	7.07E+06

LRA in-air and isothermal FFDP measurements

-9° Laser incidence

FFDP and the intensity versus VA

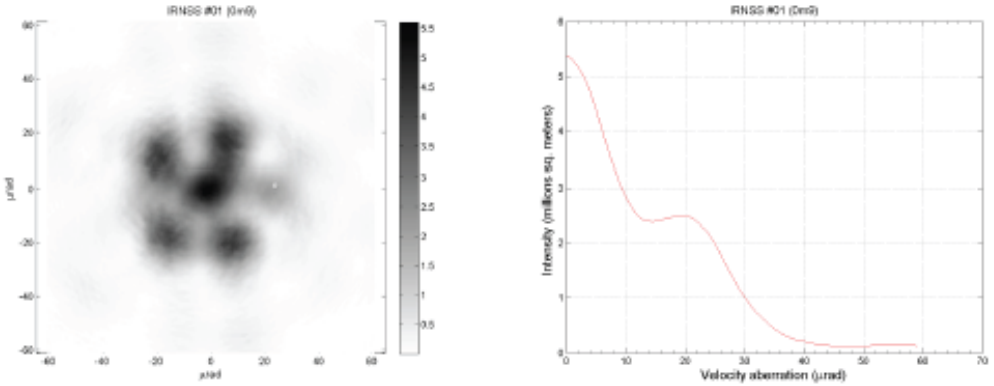

Figure 82: Left: FFDP; right: average intensity versus velocity aberration of CCRR n.01.

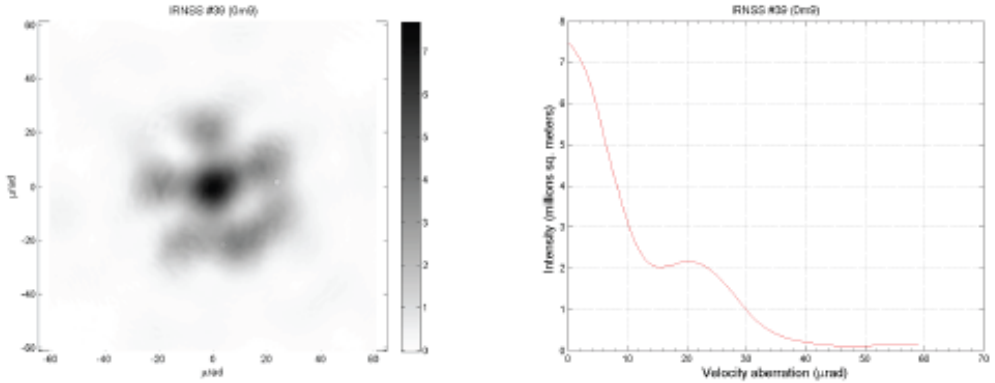

Figure 120: Left: FFDP; right: average intensity versus velocity aberration of CCRR n.39.

Table 3: Measured data of central peak intensity of every CCRRs.

ccrr_num	orientation	X [mm]	Y [mm]	Central Peak Intensity [m^2]
irn_01	-9°	0.0	0.0	5.35E+06
irn_02	-9°	26.2	45.9	6.80E+06
irn_03	-9°	78.5	45.9	8.25E+06
irn_04	-9°	104.7	0.0	2.98E+06
irn_05	-9°	78.5	-45.9	5.60E+06
irn_06	-9°	26.2	-45.9	6.70E+06
irn_07	-9°	-26.1	-45.9	5.47E+06
irn_08	-9°	-52.3	0.0	7.20E+06
irn_09	-9°	-26.1	45.9	7.20E+06
irn_10	-9°	0.0	91.8	6.70E+06
irn_11	-9°	52.4	91.8	8.64E+06
irn_12	-9°	104.7	91.8	6.61E+06
irn_13	-9°	130.9	45.9	6.35E+06
irn_14	-9°	157.1	0.0	7.10E+06
irn_15	-9°	130.9	-45.9	8.44E+06
irn_16	-9°	104.7	-91.8	8.64E+06
irn_17	-9°	52.4	-91.8	7.95E+06
irn_18	-9°	0.0	-91.8	8.03E+06
irn_19	-9°	-52.3	-91.8	4.84E+06
irn_20	-9°	-78.5	-45.9	7.09E+06
irn_21	-9°	-104.7	0.0	5.19E+06
irn_22	-9°	-78.5	45.9	6.13E+06
irn_23	-9°	-52.3	91.8	6.37E+06
irn_24	-9°	-26.1	137.7	7.41E+06
irn_25	-9°	26.2	137.7	5.93E+06
irn_26	-9°	78.5	137.7	8.00E+06
irn_27	-9°	130.9	137.7	6.78E+06
irn_28	-9°	157.1	91.8	6.92E+06
irn_29	-9°	183.2	45.9	8.09E+06
irn_30	-9°	209.4	0.0	5.90E+06
irn_31	-9°	183.2	-45.9	6.14E+06
irn_32	-9°	157.1	-91.8	3.81E+06
irn_33	-9°	130.9	-137.7	9.47E+06
irn_34	-9°	78.5	-137.7	6.33E+06
irn_35	-9°	26.2	-137.7	2.74E+06
irn_36	-9°	-26.1	-137.7	7.23E+06
irn_37	-9°	-104.7	-91.8	5.69E+06
irn_38	-9°	-104.7	91.8	8.13E+06
irn_39	-9°	209.4	91.8	7.45E+06
irn_40	-9°	209.4	-91.8	7.93E+06

LRA in-air and isothermal FFDP measurements

0° Laser incidence

We computed the intensity along a circumference at 18 µrad velocity aberration angle.

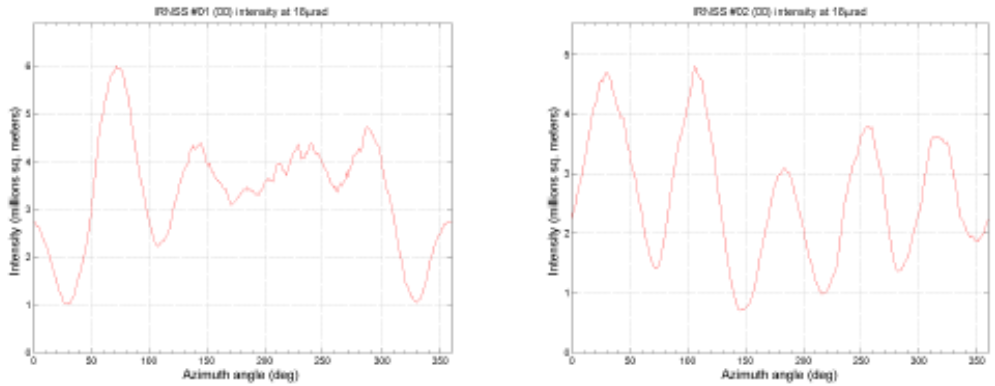

Figure 122: Left CCRR 01; right CCRR 02.

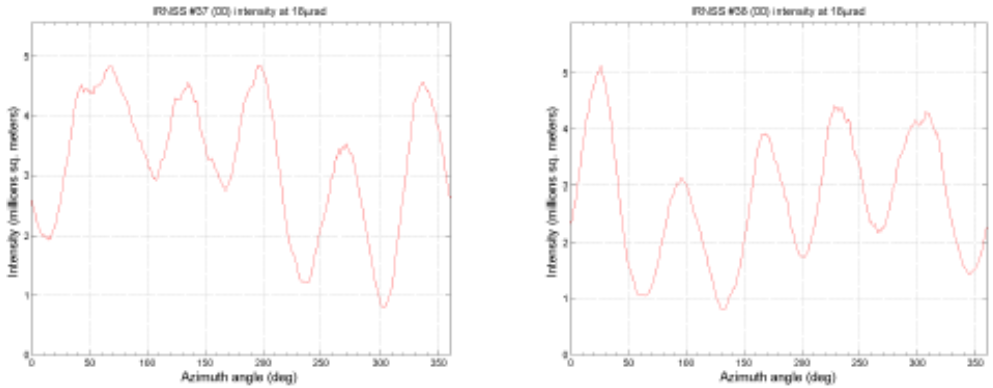

Figure 140: Left CCRR 37; right CCRR 38.

Array intensity: 118.7 x 10^6 m^2

Table 4: Measured data of maximum, minimum and average intensity at 18 µrad.

Data of maximum-minimum-average intensity at 18 µrad				
ccrr_num	orientation	Max_Int [m^2]	Min_Int [m^2]	Ave_Int [m^2]
irn_01	0°	6.01E+06	1.01E+06	3.33E+06
irn_02	0°	4.81E+06	7.05E+05	2.64E+06
irn_03	0°	4.93E+06	5.15E+05	2.42E+06
irn_04	0°	4.67E+06	1.36E+06	3.31E+06
irn_05	0°	5.44E+06	7.12E+05	3.14E+06
irn_06	0°	5.67E+06	7.56E+05	3.33E+06
irn_07	0°	5.30E+06	8.45E+05	3.10E+06
irn_08	0°	5.36E+06	3.86E+05	2.79E+06
irn_09	0°	5.07E+06	4.11E+05	2.67E+06
irn_10	0°	4.69E+06	7.41E+05	2.62E+06
irn_11	0°	5.42E+06	6.08E+05	2.74E+06
irn_12	0°	5.57E+06	4.93E+05	2.85E+06
irn_13	0°	4.77E+06	7.31E+05	3.00E+06
irn_14	0°	5.47E+06	9.79E+05	3.24E+06
irn_15	0°	5.16E+06	6.56E+05	2.82E+06
irn_16	0°	5.20E+06	2.97E+05	2.73E+06
irn_17	0°	4.33E+06	4.38E+05	2.59E+06
irn_18	0°	4.61E+06	5.74E+05	2.63E+06
irn_19	0°	6.16E+06	4.18E+05	3.28E+06
irn_20	0°	5.31E+06	1.13E+06	3.22E+06
irn_21	0°	5.23E+06	6.19E+05	3.22E+06
irn_22	0°	5.09E+06	1.03E+06	3.12E+06
irn_23	0°	6.09E+06	6.00E+05	2.92E+06
irn_24	0°	6.12E+06	6.66E+05	3.13E+06
irn_25	0°	5.28E+06	1.13E+06	3.35E+06
irn_26	0°	6.06E+06	4.79E+05	2.75E+06
irn_27	0°	5.36E+06	6.17E+05	3.11E+06
irn_28	0°	4.79E+06	7.24E+05	2.87E+06
irn_29	0°	4.16E+06	9.21E+05	2.45E+06
irn_30	0°	5.82E+06	9.11E+05	3.12E+06
irn_31	0°	5.02E+06	4.98E+05	2.88E+06
irn_32	0°	6.29E+06	1.20E+06	3.69E+06
irn_33	0°	5.16E+06	7.98E+05	2.47E+06
irn_34	0°	4.67E+06	1.03E+06	3.07E+06
irn_35	0°	6.76E+06	1.35E+06	3.36E+06
irn_36	0°	5.19E+06	3.80E+05	2.98E+06
irn_37	0°	4.85E+06	7.95E+05	3.25E+06
irn_38	0°	5.14E+06	8.02E+05	2.77E+06
irn_39	0°	5.85E+06	6.47E+05	2.89E+06
irn_40	0°	5.64E+06	3.02E+05	2.83E+06

LRA in-air and isothermal FFDP measurements

+9° Laser incidence

We computed the intensity along a circumference at 18 µrad velocity aberration angle.

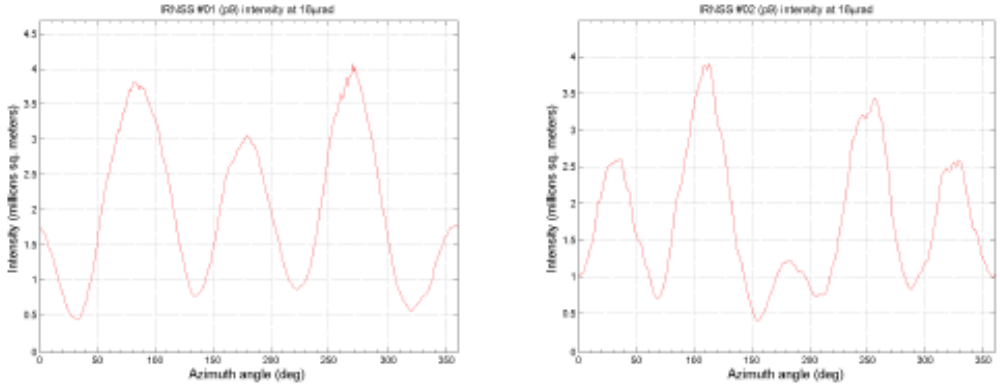

Figure 142: Left CCRR 01; right CCRR 02.

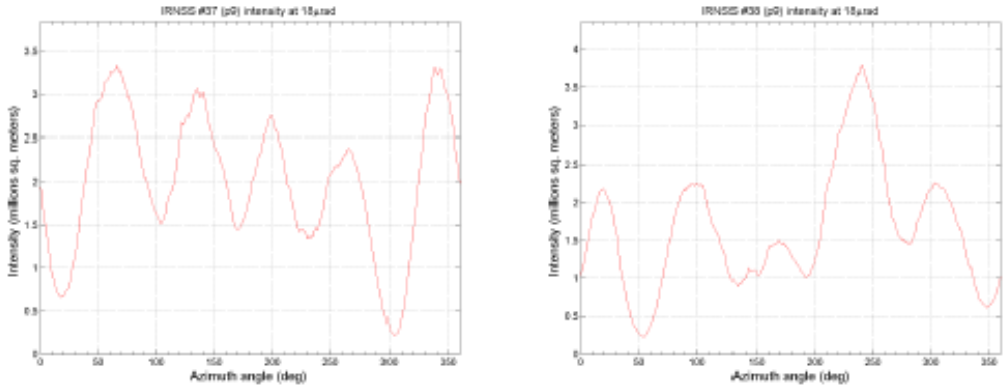

Figure 160: Left CCRR 37; right CCRR 38.

Array intensity: 82.6 x 10^6 m^2

Table 5: Measured data of maximum, minimum and average intensity at 18 µrad.

Data of maximum-minimum-average intensity at 18 µrad				
ccrr_num	orientation	Max_Int [m^2]	Min_Int [m^2]	Ave_Int [m^2]
irn_01	+9°	4.08E+06	4.44E+05	1.97E+06
irn_02	+9°	3.91E+06	3.90E+05	1.79E+06
irn_03	+9°	3.51E+06	3.46E+05	1.68E+06
irn_04	+9°	4.41E+06	9.58E+05	2.35E+06
irn_05	+9°	3.70E+06	9.62E+05	2.11E+06
irn_06	+9°	3.80E+06	2.33E+05	2.12E+06
irn_07	+9°	4.51E+06	6.61E+05	2.15E+06
irn_08	+9°	3.56E+06	1.46E+05	1.85E+06
irn_09	+9°	4.16E+06	3.79E+05	2.06E+06
irn_10	+9°	3.15E+06	2.25E+05	1.81E+06
irn_11	+9°	4.00E+06	3.56E+05	1.81E+06
irn_12	+9°	3.81E+06	2.13E+05	1.80E+06
irn_13	+9°	4.09E+06	5.24E+05	2.00E+06
irn_14	+9°	3.74E+06	3.65E+05	1.83E+06
irn_15	+9°	2.83E+06	1.50E+05	1.73E+06
irn_16	+9°	3.11E+06	1.54E+05	1.82E+06
irn_17	+9°	3.15E+06	1.80E+05	1.89E+06
irn_18	+9°	3.73E+06	4.09E+05	1.78E+06
irn_19	+9°	4.41E+06	2.22E+05	2.08E+06
irn_20	+9°	3.34E+06	1.39E+05	1.88E+06
irn_21	+9°	4.47E+06	5.84E+05	2.15E+06
irn_22	+9°	3.99E+06	2.15E+05	2.08E+06
irn_23	+9°	3.98E+06	2.65E+05	1.85E+06
irn_24	+9°	4.68E+06	3.12E+05	1.94E+06
irn_25	+9°	4.01E+06	5.04E+05	1.91E+06
irn_26	+9°	3.82E+06	5.46E+05	1.94E+06
irn_27	+9°	3.07E+06	1.73E+05	1.74E+06
irn_28	+9°	3.30E+06	3.18E+05	1.93E+06
irn_29	+9°	3.47E+06	5.17E+05	1.69E+06
irn_30	+9°	3.32E+06	1.36E+05	1.85E+06
irn_31	+9°	3.57E+06	5.09E+05	2.20E+06
irn_32	+9°	4.14E+06	6.43E+05	2.40E+06
irn_33	+9°	3.03E+06	2.87E+05	1.62E+06
irn_34	+9°	3.26E+06	3.26E+05	1.93E+06
irn_35	+9°	4.22E+06	3.95E+05	2.10E+06
irn_36	+9°	3.25E+06	1.68E+05	1.85E+06
irn_37	+9°	3.34E+06	2.16E+05	2.02E+06
irn_38	+9°	3.79E+06	2.25E+05	1.66E+06
irn_39	+9°	3.27E+06	4.17E+05	1.74E+06
irn_40	+9°	3.14E+06	2.42E+05	1.49E+06

LRA in-air and isothermal FFDP measurements

-9° Laser incidence

We computed the intensity along a circumference at 18 µrad velocity aberration angle.

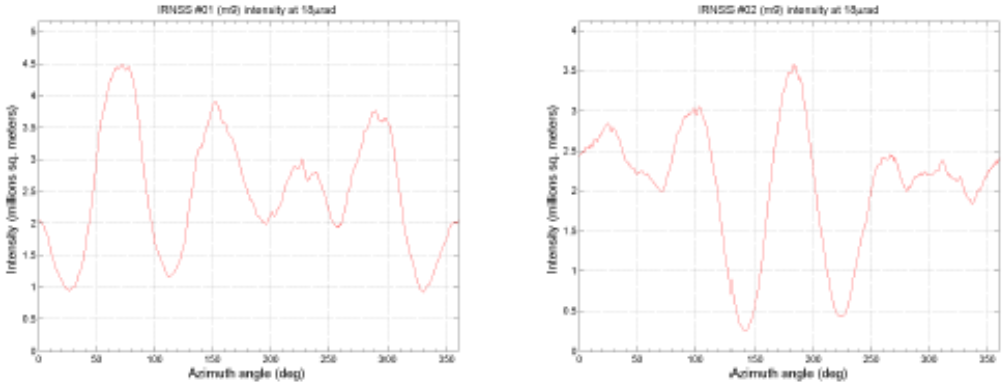

Figure 162: Left CCRR 01; right CCRR 02.

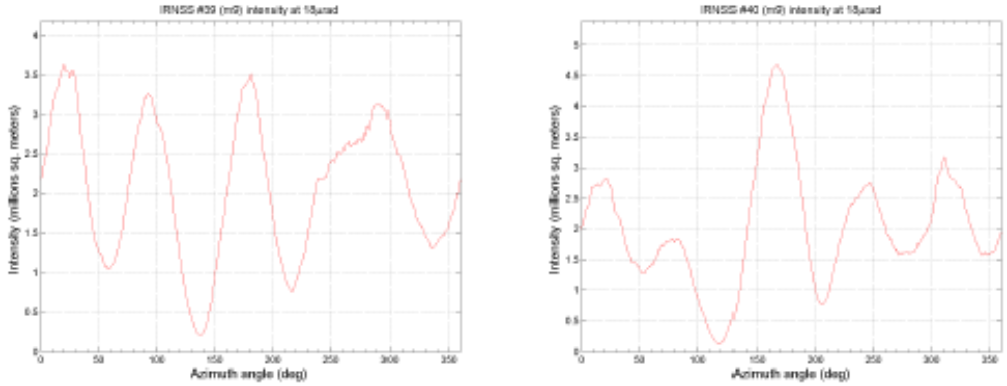

Figure 180: Left CCRR 37; right CCRR 38.

Data of maximum-minimum-average intensity at 18 µrad				
ccrr_num	orientation	Max_Int [m^{-2}]	Min_Int [m^{-2}]	Ave_Int [m^{-2}]
irn_01	-9°	4.49E+06	9.21E+05	2.48E+06
irn_02	-9°	3.58E+06	2.53E+05	2.08E+06
irn_03	-9°	3.78E+06	3.86E+05	1.78E+06
irn_04	-9°	3.95E+06	3.82E+05	2.38E+06
irn_05	-9°	3.86E+06	2.61E+05	2.17E+06
irn_06	-9°	5.10E+06	3.83E+05	2.31E+06
irn_07	-9°	3.44E+06	1.51E+05	2.11E+06
irn_08	-9°	3.74E+06	4.98E+05	2.02E+06
irn_09	-9°	2.92E+06	2.85E+05	1.70E+06
irn_10	-9°	4.47E+06	4.07E+05	1.95E+06
irn_11	-9°	3.16E+06	2.05E+05	1.71E+06
irn_12	-9°	3.77E+06	1.46E+05	1.89E+06
irn_13	-9°	3.29E+06	2.32E+05	2.17E+06
irn_14	-9°	4.76E+06	3.93E+05	2.01E+06
irn_15	-9°	3.83E+06	2.42E+05	2.00E+06
irn_16	-9°	3.95E+06	3.17E+05	1.94E+06
irn_17	-9°	3.34E+06	2.53E+05	2.01E+06
irn_18	-9°	3.00E+06	1.58E+05	1.78E+06
irn_19	-9°	3.82E+06	1.39E+05	2.04E+06
irn_20	-9°	4.12E+06	5.60E+05	2.15E+06
irn_21	-9°	3.97E+06	2.47E+05	2.11E+06
irn_22	-9°	3.39E+06	4.03E+05	2.11E+06
irn_23	-9°	3.64E+06	2.04E+05	1.69E+06
irn_24	-9°	4.07E+06	2.02E+05	1.90E+06
irn_25	-9°	3.43E+06	2.47E+05	2.21E+06
irn_26	-9°	3.26E+06	3.28E+05	1.70E+06
irn_27	-9°	3.76E+06	8.41E+05	2.24E+06
irn_28	-9°	3.43E+06	3.80E+05	2.15E+06
irn_29	-9°	2.99E+06	2.47E+05	1.76E+06
irn_30	-9°	4.46E+06	9.39E+05	2.51E+06
irn_31	-9°	4.10E+06	3.94E+05	2.36E+06
irn_32	-9°	4.60E+06	2.49E+05	2.33E+06
irn_33	-9°	4.14E+06	1.30E+05	1.87E+06
irn_34	-9°	3.69E+06	4.92E+05	2.19E+06
irn_35	-9°	4.82E+06	5.35E+05	2.49E+06
irn_36	-9°	3.90E+06	3.12E+05	1.91E+06
irn_37	-9°	4.23E+06	4.23E+05	2.40E+06
irn_38	-9°	3.71E+06	2.20E+05	1.87E+06
irn_39	-9°	3.63E+06	1.95E+05	2.09E+06
irn_40	-9°	4.68E+06	1.31E+05	2.03E+06

Array intensity: 76.6 x 10^6 m^2

LRA in-air and isothermal FFDP measurements

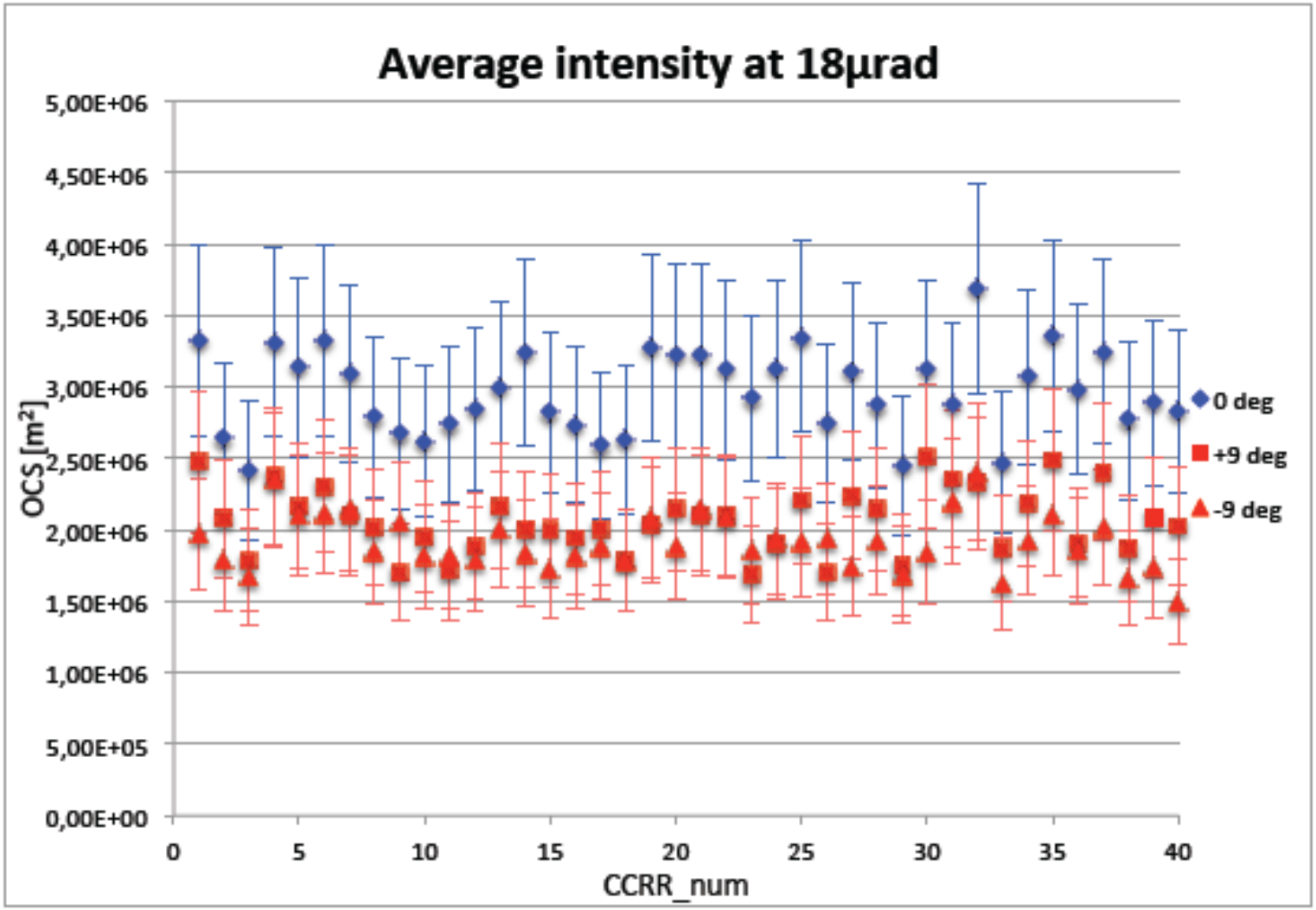

Figure 182: average intensity at 18µrad for 0 degrees (blu rhombus), +9 degrees (red square) , -9 degrees (red triangle) inclination angle.

Average intensity at 18µrad for 0°, +9°, -9° inclination angle together, using the values The error bars (20% of the relative intensity value), take into account the optical circuit aberrations.

LRA SCF-Test n.1: fixed temperature and no Sun Simulator @ -85°C

Test structure:

- FFDP measurements of all the CCRRs of the IRNSS LRA done at -85°C in space conditions without Sun Simulator.
- Measurements on the 40 CCRRs have been repeated for three different inclination angles: with array in front of the laser window, namely 0 degrees, and ±9 degrees laser incidence (same sign convention as previously stated).
- We set up the starting condition defined in [AD-2]: array was kept in the space environment of the SCF with the temperature of the plate kept at -85°C. As the temperatures of the different parts reached a steady state we started the measurement.
- We acquire the CCRR energy distribution of both the polarization components, horizontal and vertical.

Analysis:

- Analysis of raw optical measured data with a dedicated MATLAB program.
- For each tested CCRR and laser incidence angle the program computes:
  - The Field Diffraction Pattern (FFDP) in Optical Cross Section (OCS) unit.
  - OCS intensity distribution versus velocity aberration.
  - OCS intensity distribution in annulus at 18 µrad velocity aberration.
  - Average OCS intensity at 18 µrad velocity aberration a total CCRR FFDP.

LRA SCF-Test n.1: fixed temperature and no Sun Simulator @ -85°C

0° Laser incidence

FFDP and the intensity versus VA.

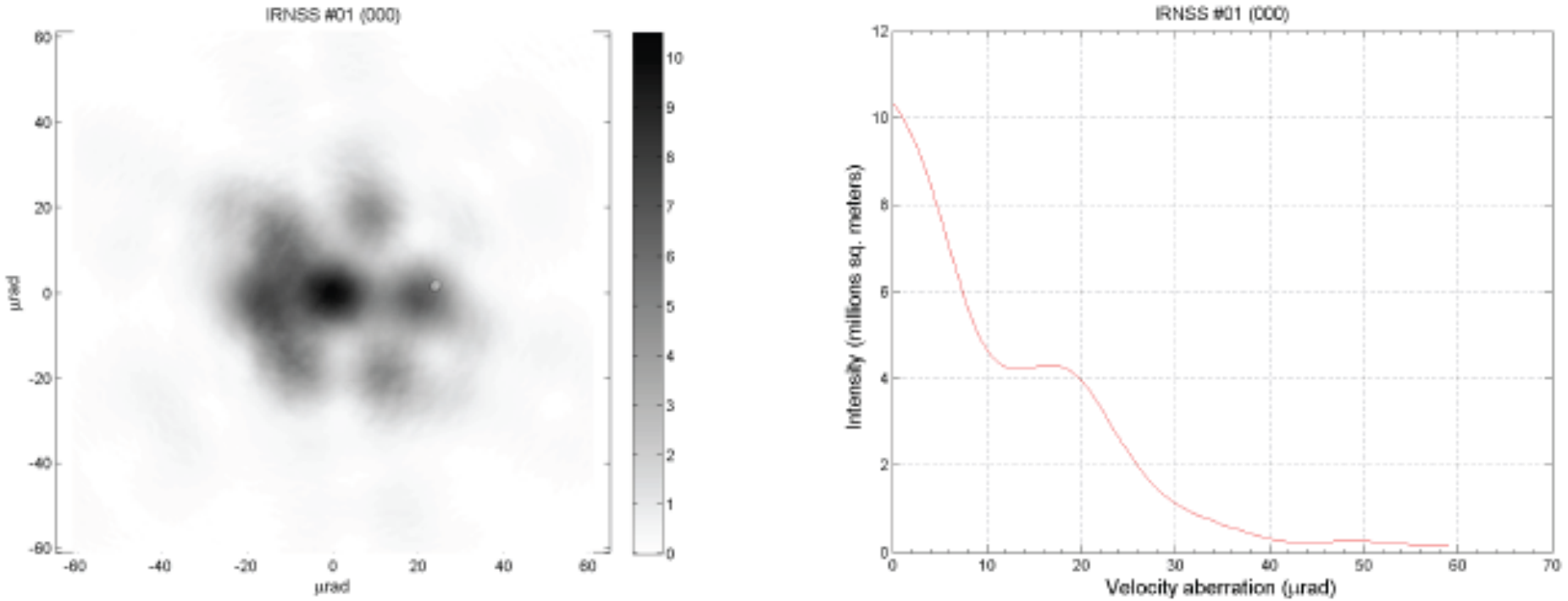

Figure 2:Left: FFDP; right: average intensity versus velocity aberration of CCRR n.01.

LRA SCF-Test n.1: fixed temperature and no Sun Simulator @ -85°C

+9° Laser incidence

FFDP and the intensity versus VA.

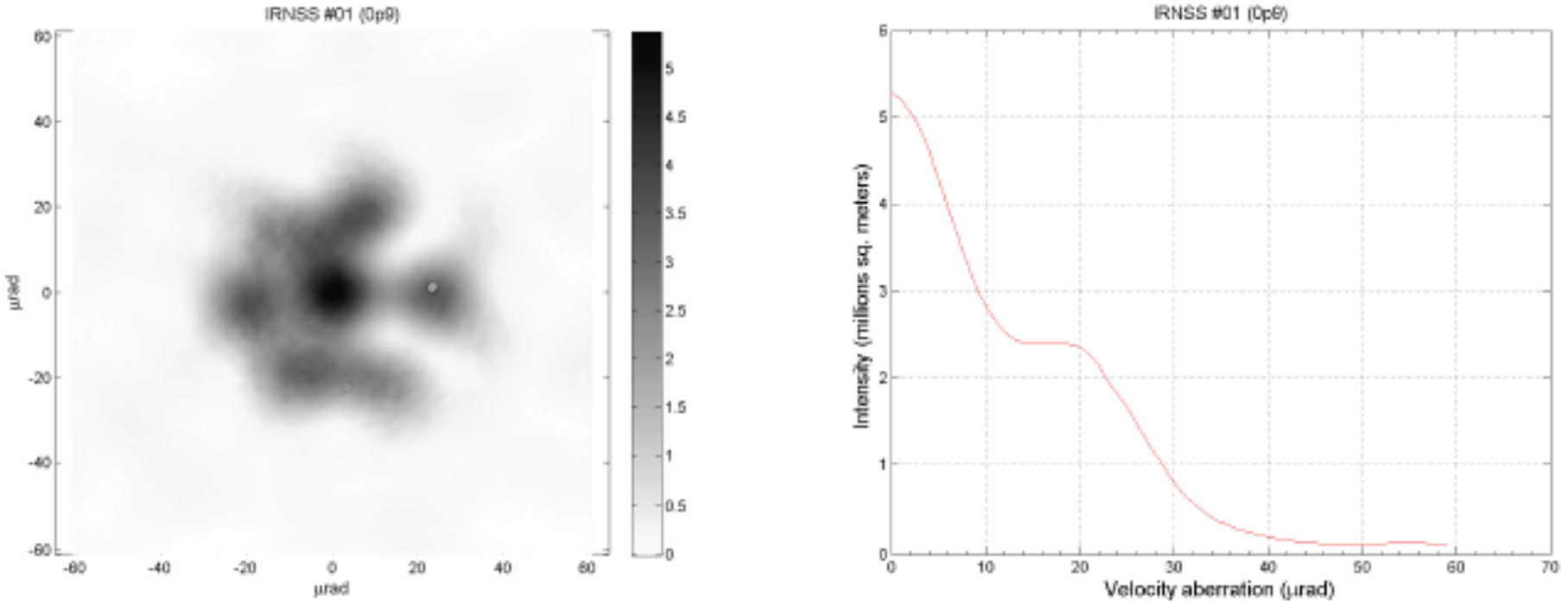

Figure 42: Left: FFDP; right: average intensity versus velocity aberration of CCRR n.01.

LRA SCF-Test n.1: fixed temperature and no Sun Simulator @ -85°C

-9° Laser incidence

FFDP and the intensity versus VA.

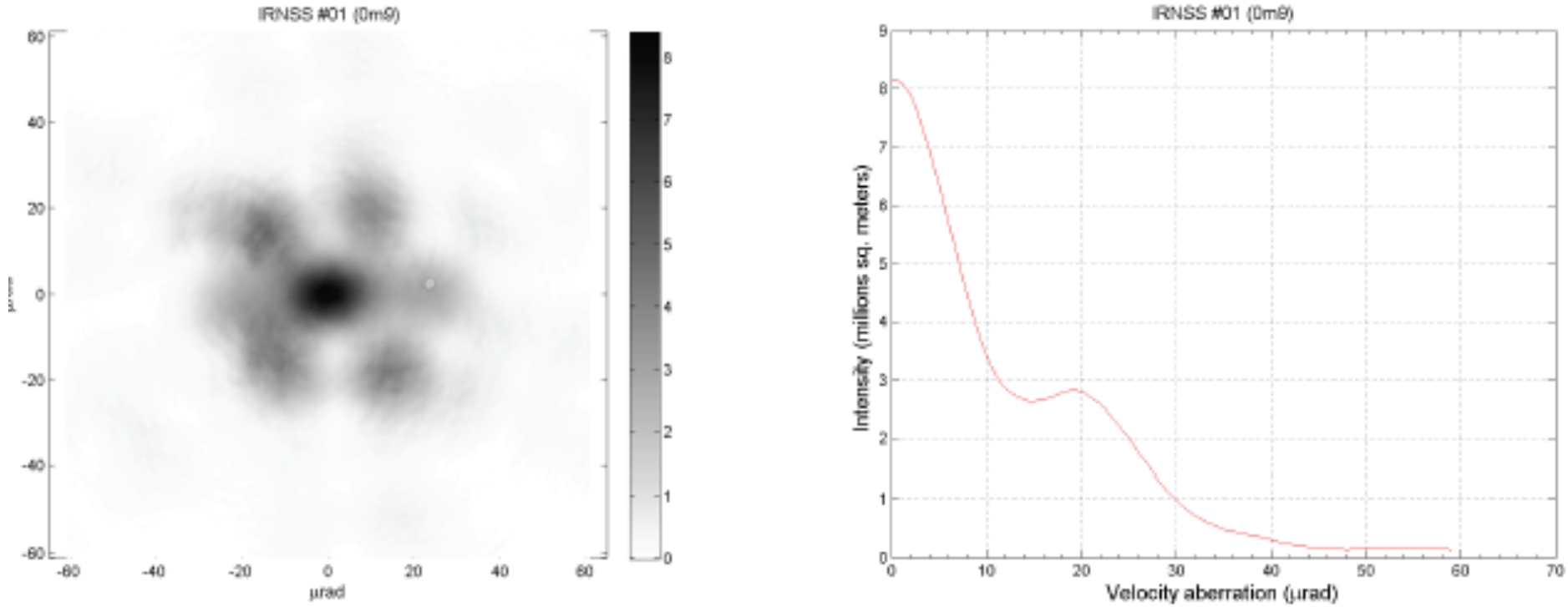

Figure 82: Left: FFDP; right: average intensity versus velocity aberration of CCRR n.01.

LRA SCF-Test n.1: fixed temperature and no Sun Simulator @ -85°C

0° Laser incidence

We computed the intensity along a circumference at 18 µrad velocity aberration angle.

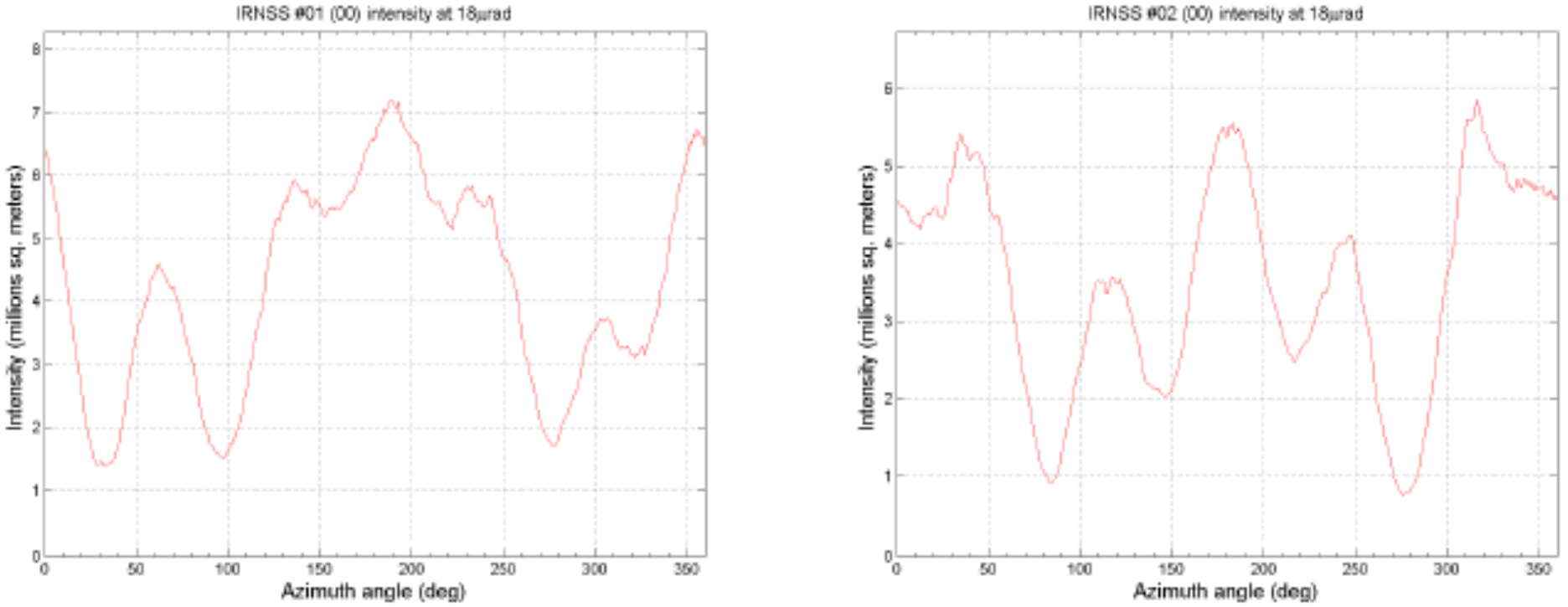

Figure 122: Left CCRR 01; right CCRR 02.

Array intensity: 132.4 x 10^6 m^2

LRA SCF-Test n.1: fixed temperature and no Sun Simulator @ -85°C

+9° Laser incidence

We computed the intensity along a circumference at 18 µrad velocity aberration angle.

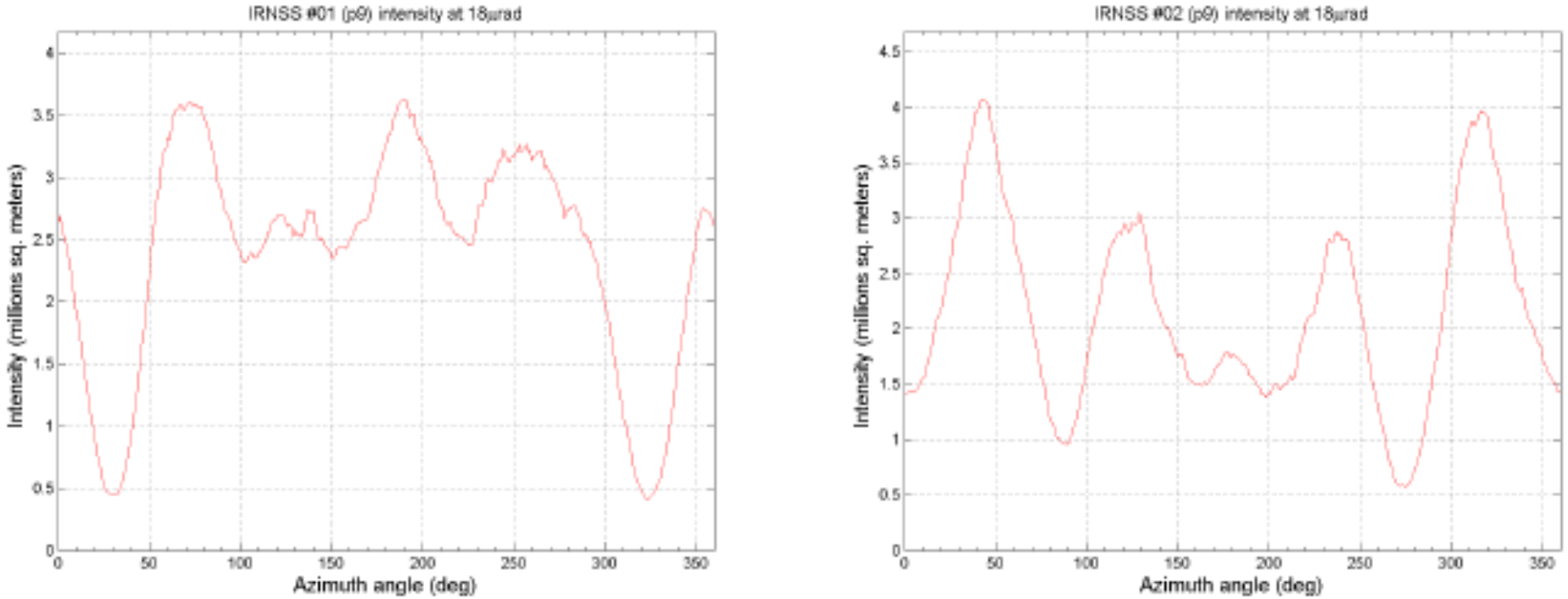

Figure 142: Left CCRR 01; right CCRR 02.

Array intensity: 95.2 x 10^6 m^2

LRA SCF-Test n.1: fixed temperature and no Sun Simulator @ -85°C

-9° Laser incidence

We computed the intensity along a circumference at 18 µrad velocity aberration angle.

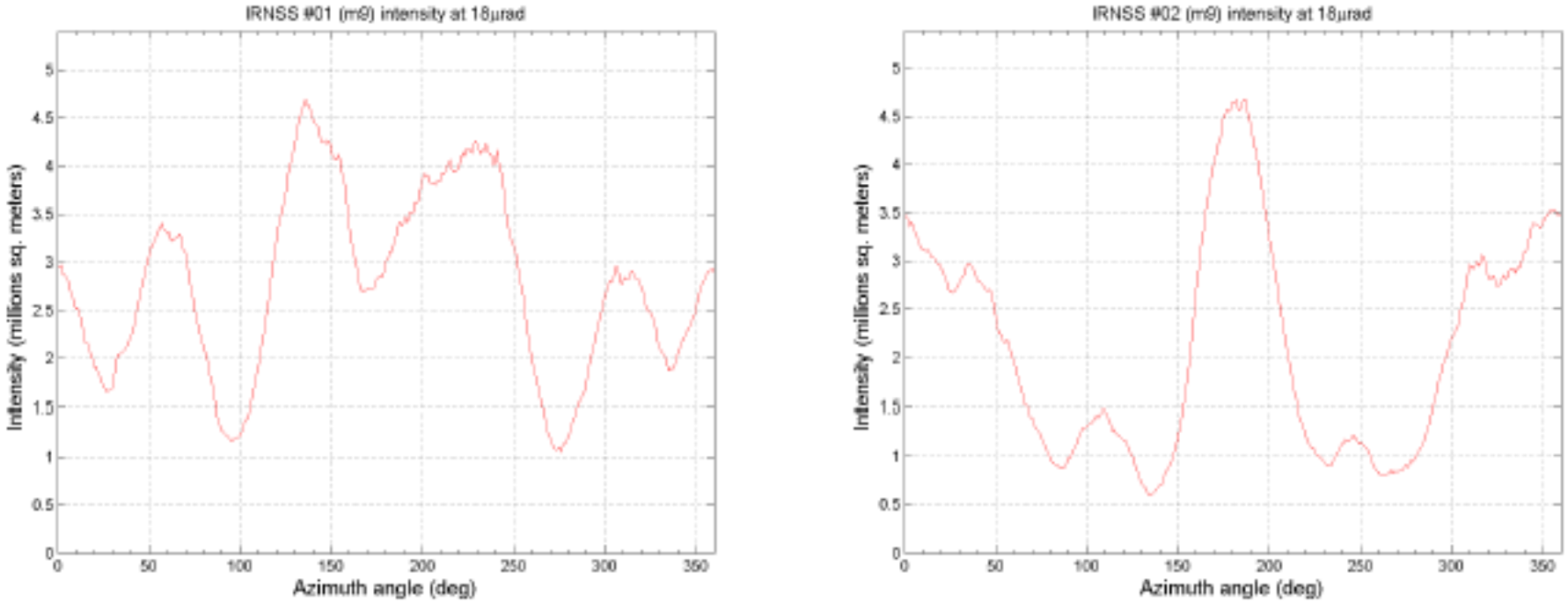

Figure 162: Left CCRR 01; right CCRR 02.

Array intensity: 84.3 x 10^6 m^2

LRA SCF-Test n.1: fixed temperature and no Sun Simulator @ -85°C

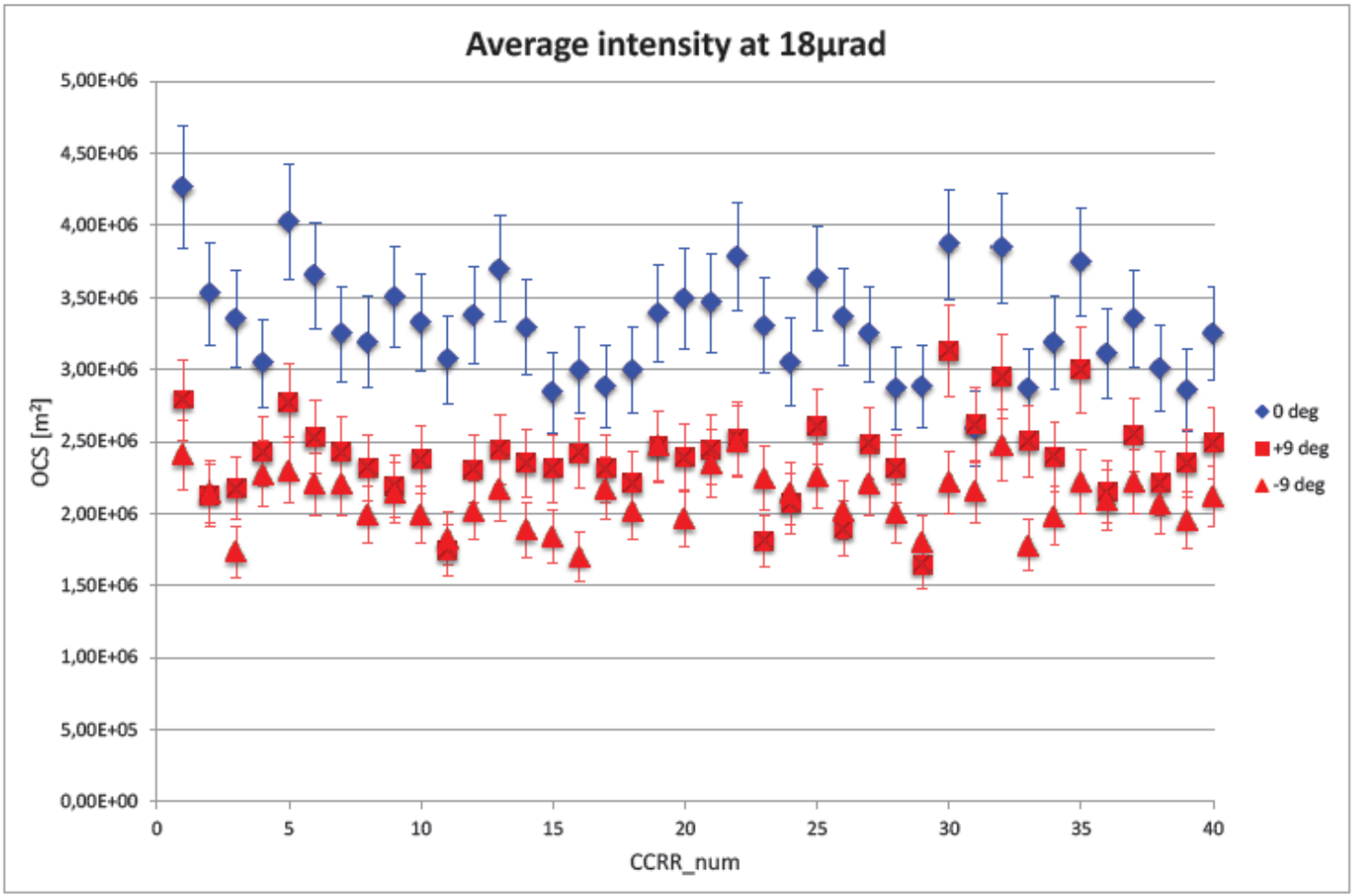

Figure 182: average intensity at 18µrad for 0 degrees (blue rhombus), +9 degrees (red square) , -9 degrees (red triangle) inclination angle.

Average intensity at 18µrad for 0°, +9°, -9° inclination angle together, using the values The error bars (20% of the relative intensity value), take into account the optical circuit aberrations.

LRA SCF-Test n.1: fixed temperature and no Sun Simulator @ -85°C

Conclusion: FFDPs in a stationary space environment (no Sun Simulator) do not differ too much from those in air and isothermal conditions.
All FFDP intensities are slightly increased (by about 10%, wrt in-air/stp conds), due to different (though stationary) environment conditions.
In both cases we have that:

- FFDPs at +9° and -9° have the same level of intensity, within errors.
- FFDP intensities at 0° are ~30% more intense than those at ±9°.

LRA SCF-Test n.1: fixed temperature and no Sun Simulator @ 105°C

Test structure:

- FFDP measurements of all the CCRRs of the IRNSS LRA done at 105°C in space conditions without Sun Simulator.
- Measurements on the 40 CCRRs have been repeated for three different inclination angles: with array in front of the laser window, namely 0 degrees, and ±9 degrees laser incidence (plus sign counter clockwise rotation).
- We set up the starting condition defined in [AD-2]: array was kept in the space environment of the SCF with the temperature of the plate kept at 105°C. As the temperatures of the different parts reached a steady state we started the measurement.
- We acquire the CCRR energy distribution of both the polarization components, horizontal and vertical.

Analysis:

- Analysis of raw optical measured data with a dedicated MATLAB program.
- For each tested CCRR and laser incidence angle the program computes:
  - The Field Diffraction Pattern (FFDP) in Optical Cross Section (OCS) unit.
  - OCS intensity distribution versus velocity aberration.
  - OCS intensity distribution in annulus at 18 µrad velocity aberration.
  - Average OCS intensity at 18 µrad velocity aberration a total CCRR FFDP.

LRA SCF-Test n.1: fixed temperature and no Sun Simulator @ 105°C

0° Laser incidence

FFDP and the intensity versus VA.

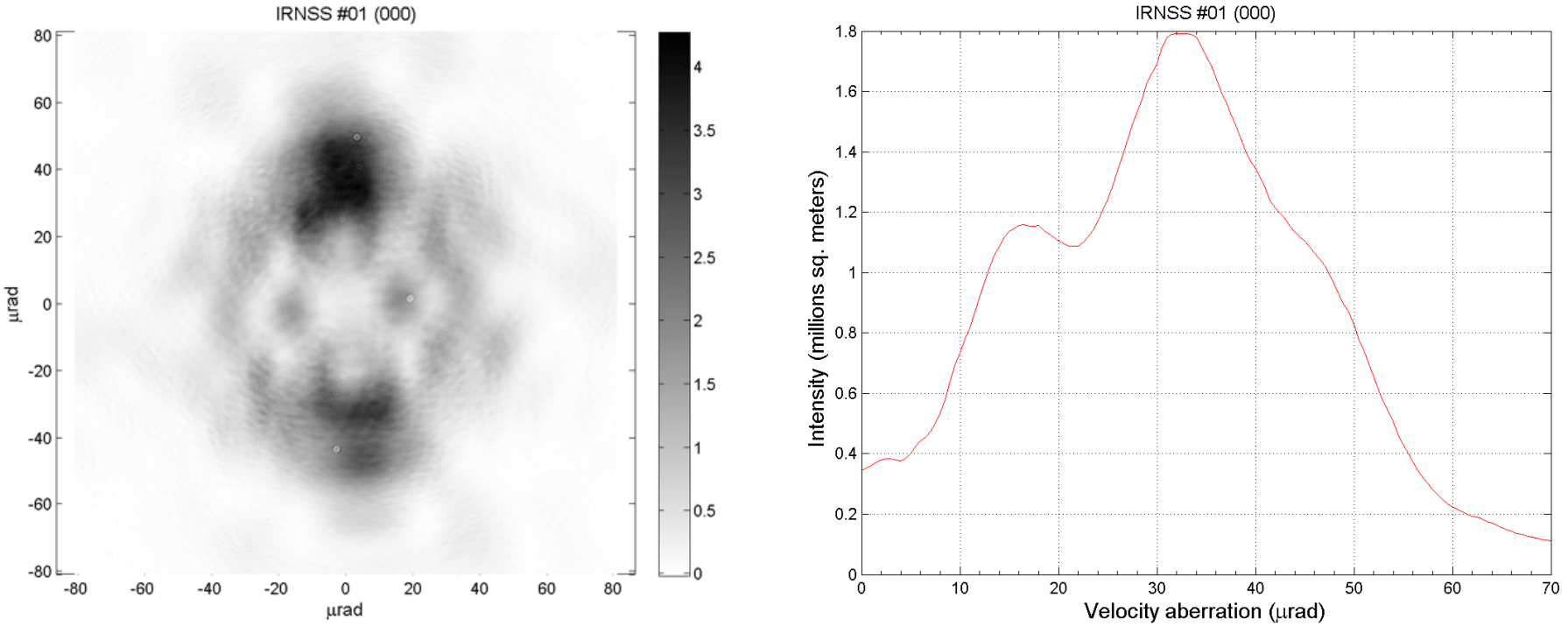

Figure 183: Left: FFDP; right: average intensity versus velocity aberration of CCRR n.01.

LRA SCF-Test n.1: fixed temperature and no Sun Simulator @ 105°C

+9° Laser incidence

FFDP and the intensity versus VA.

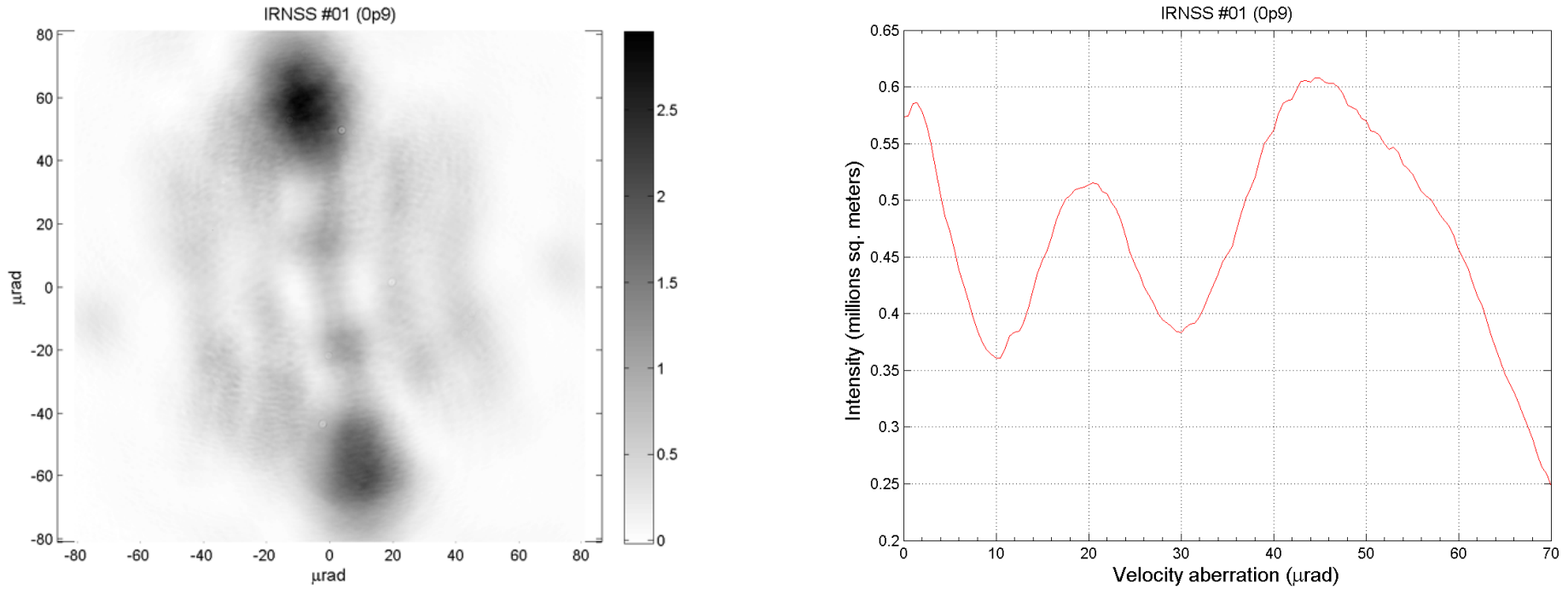

Figure 224: Left: FFDP; right: average intensity versus velocity aberration of CCRR n.01.

LRA SCF-Test n.1: fixed temperature and no Sun Simulator @ 105°C

-9° Laser incidence

FFDP and the intensity versus VA.

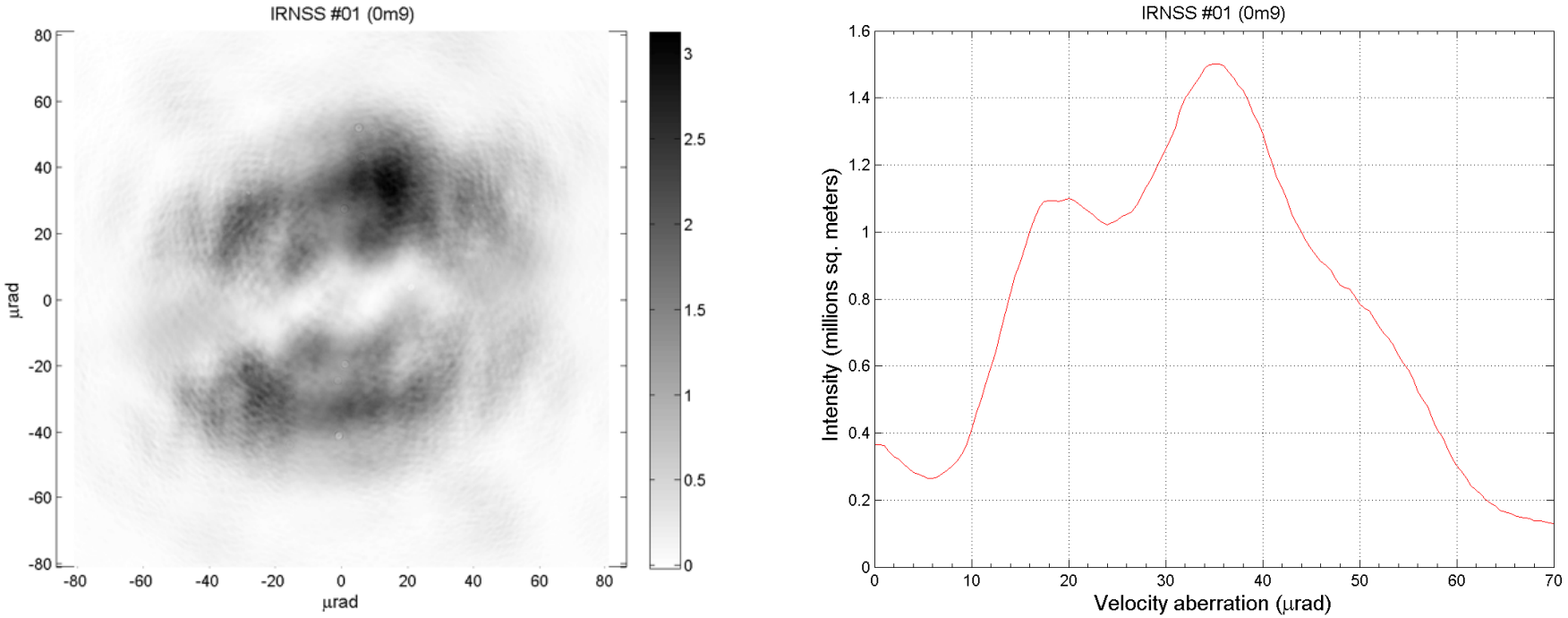

Figure 264: Left: FFDP; right: average intensity versus velocity aberration of CCRR n.01.

LRA SCF-Test n.1: fixed temperature and no Sun Simulator @ 105°C

0° Laser incidence

We computed the intensity along a circumference at 18 µrad velocity aberration angle.

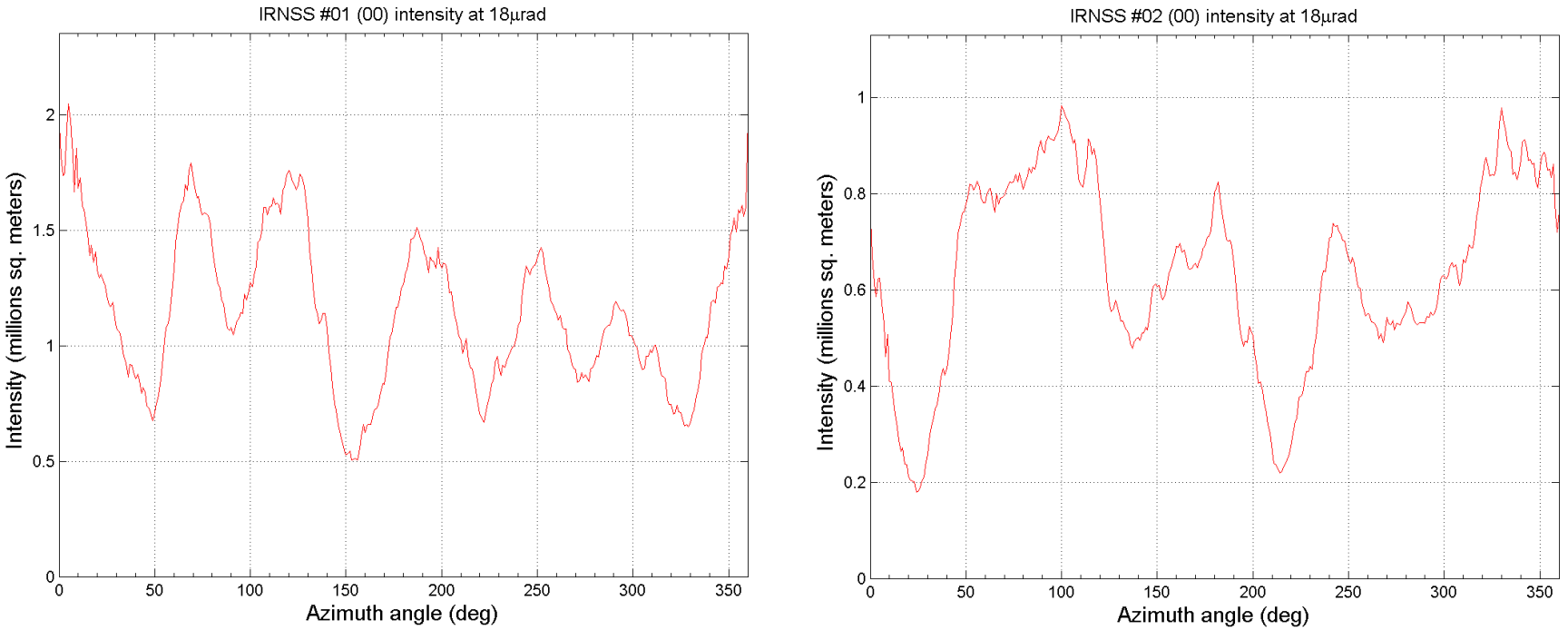

Figure 304: Left CCRR 01; right CCRR 02.

Array intensity: 31.7 x 10^6 m^2

LRA SCF-Test n.1: fixed temperature and no Sun Simulator @ 105°C

+9° Laser incidence

We computed the intensity along a circumference at 18 µrad velocity aberration angle.

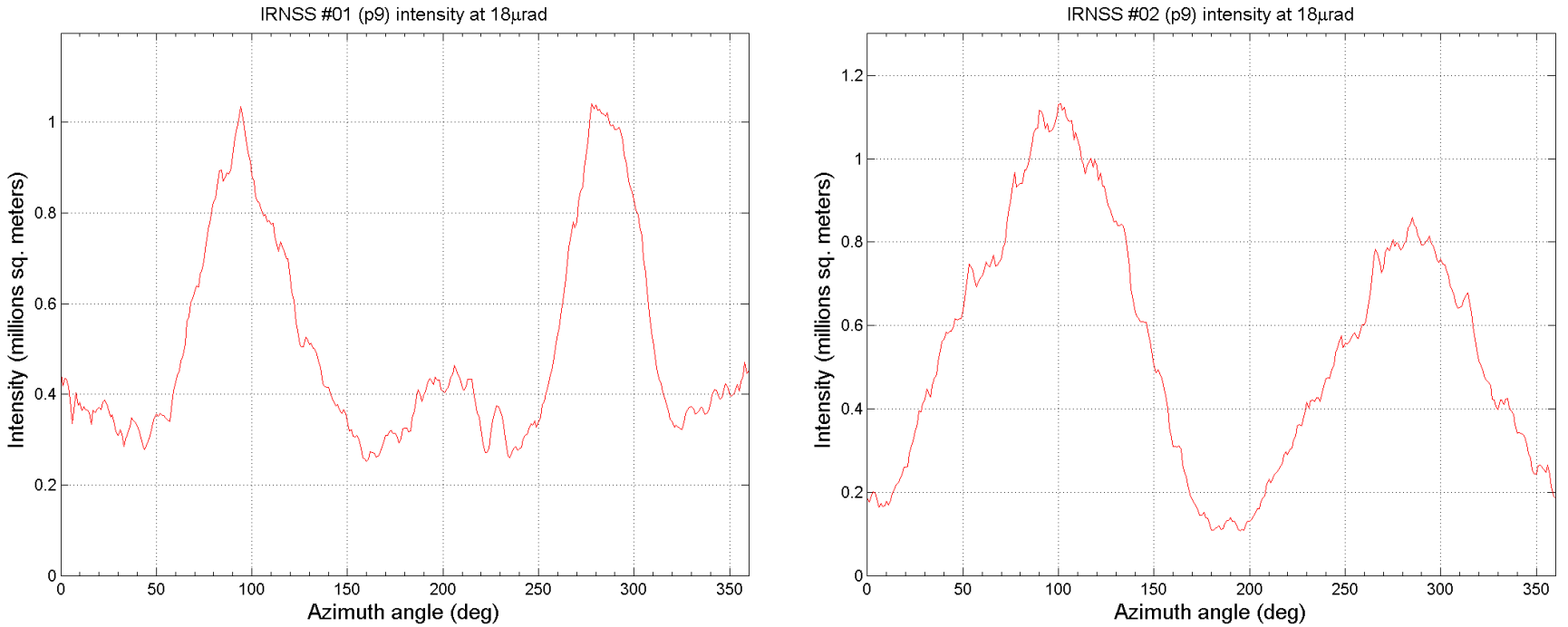

Figure 324: Left CCRR 01; right CCRR 02.

Array intensity: 27.6 x 10^6 m^2

LRA SCF-Test n.1: fixed temperature and no Sun Simulator @ 105°C

-9° Laser incidence

We computed the intensity along a circumference at 18 µrad velocity aberration angle.

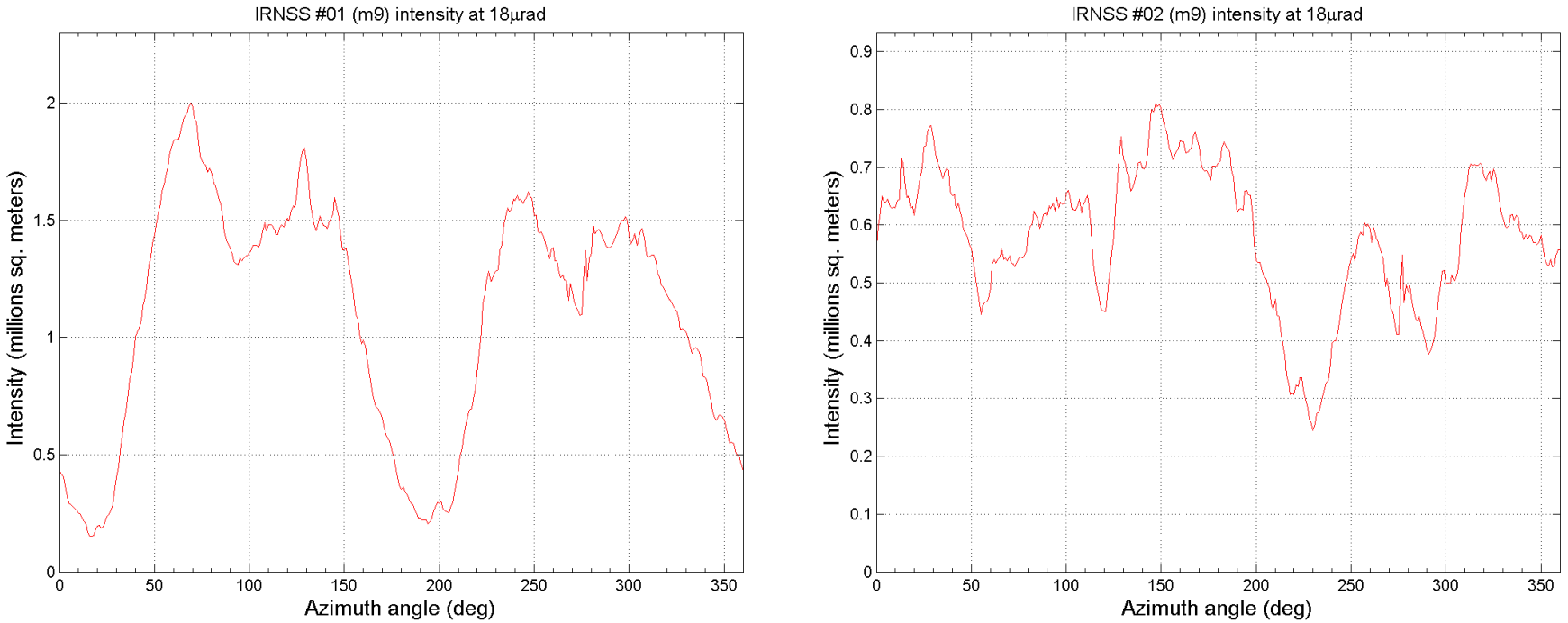

Figure 344: Left CCRR 01; right CCRR 02.

Array intensity: 29.9 x 10^6 m^2

LRA SCF-Test n.1: fixed temperature and no Sun Simulator @ 105°C

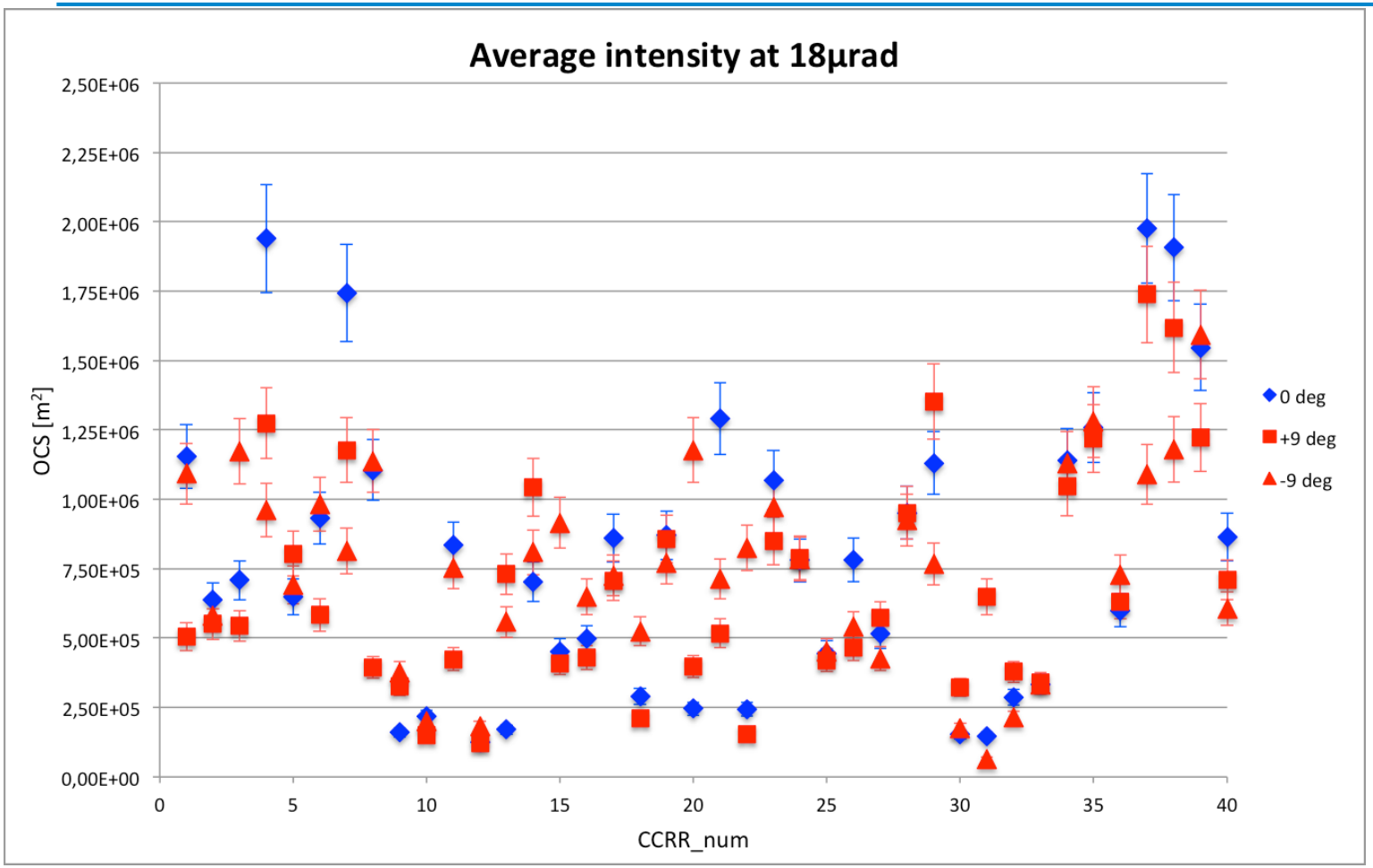

Average intensity at 18µrad for 0°, +9°, -9° inclination angle together, using the values The error bars (20% of the relative intensity value), take into account the optical circuit aberrations.

Figure 364: average intensity at 18µrad for 0 degrees (blue diamond), +9 degrees (red square) , -9 degrees (red triangle) inclination angle.

LRA SCF-Test n.1: fixed temperature and no Sun Simulator @ 105°C

Conclusion: CCRRs show clearly two distinct behaviors at the two temperatures, caused by the temperature difference between the array tray and the chamber environment. In fact as the tray is kept at -85°C, the temperature gradient inside the CCRRs is contained, thus resulting in FFDPs rather similar with respect to in air FFDP measurements; on the contrary keeping the tray at 105°C with the environment at -175°C, inside the CCRRs a high temperature gradient arises, modifying considerably the optical return of the CCRRs.

With the temperature of the tray set at 105°C, FFDPs change dramatically; the majority of the intensity is moved away from the center and the overall intensity is decreased. Average intensities at high temp is 2.5-3 times lower than the case at low temperature and, there seems to be no difference among average intensity of FFDPs with the array orthogonal to the laser and those with the array kept at 9° and -9°, as shown in Figure 364.

LRA SCF-Test n.2: Sun Simulator at varying angles

Test Structure:

- Sun Simulator illuminating the array at changing angles, exploiting the rotation system of the SCF, with a rate of about 15˚/hour.
- Waited until the payload and the surrounding environment reached the starting equilibrium conditions (cold/vacuum and LRA tray at Ti=20˚C).
- Start with an automatic procedure which lasted 6 hours.
- FFDPs and IR pictures of each measured CCRR (x5).
- Extra valuable data and deliverables (not foreseen by [AD-1]) in order to better understand the optical and thermal behaviour of the array:
  1. Two FFDPs more than what planned in [AD-1] (one FFDP at the beginning and one at the end of the orbit).
  2. Thermal analysis based on IR pictures taken together with FFDPs.

Optical Analysis:

- Analysis of raw optical measured data with a dedicated MATLAB program.
- For each tested CCRR and laser incidence angle the program computes:
  - The Field Diffraction Pattern (FFDP) in Optical Cross Section (OCS) unit.
  - OCS intensity distribution versus velocity aberration.
  - OCS intensity distribution in annulus at 18 µrad velocity aberration.
  - Average OCS intensity at 18 µrad velocity aberration a total CCRR FFDP.

LRA SCF-Test n.2: Sun Simulator at varying angles - optical analysis

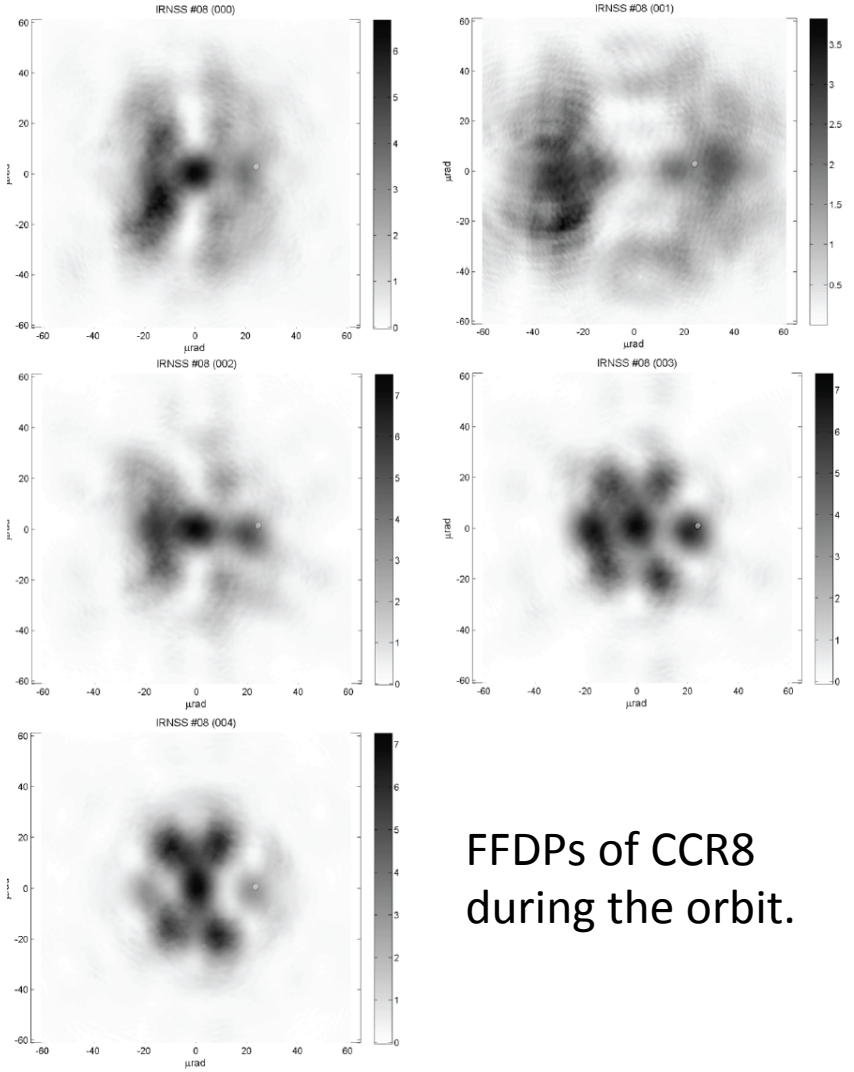

FFDPs of CCR8 during the orbit.

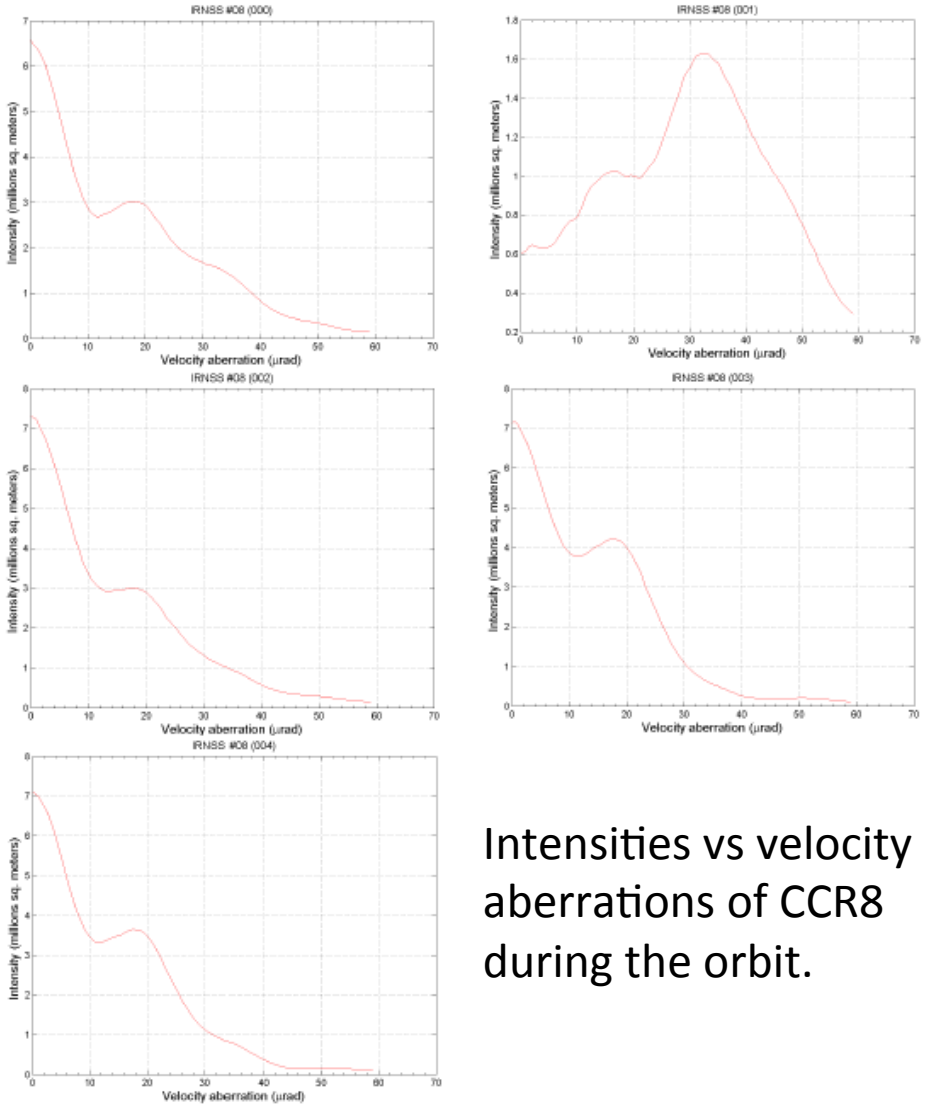

Intensities vs velocity aberrations of CCR8 during the orbit.

LRA SCF-Test n.2: Sun Simulator at varying angles - optical analysis

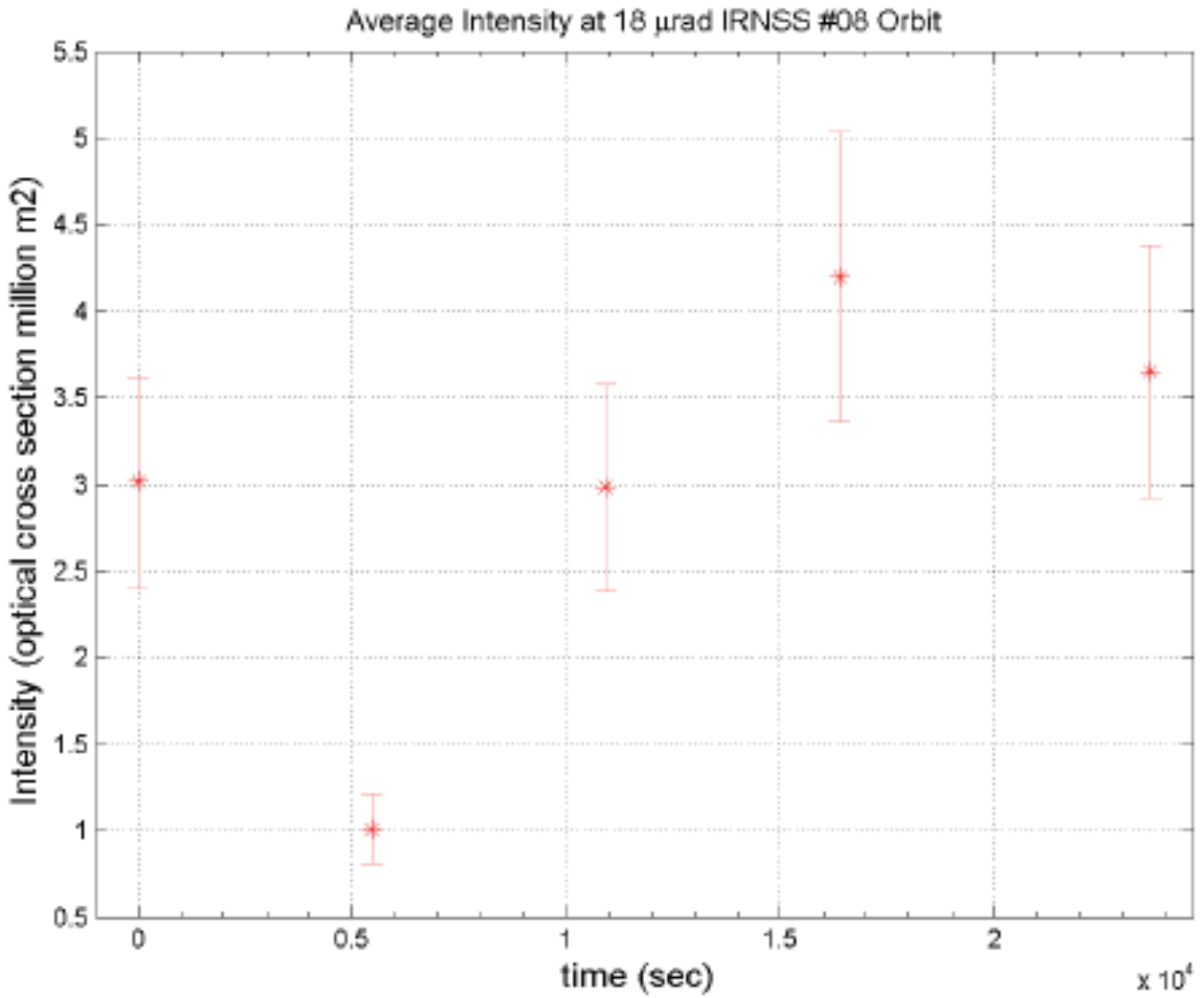

Figure 7 Average intensity variation of CCRR 8 at 18 µrad during orbit. Error on intensity is 20% of the relative intensity

LRA SCF-Test n.2: Sun Simulator at varying angles - thermal analysis

Same things done also for CCRs n. 9, 12, 13, 21, 22, 28, 29.

LRA SCF-Test n.2: Sun Simulator at varying angles - optical analysis for all 8 CCRs

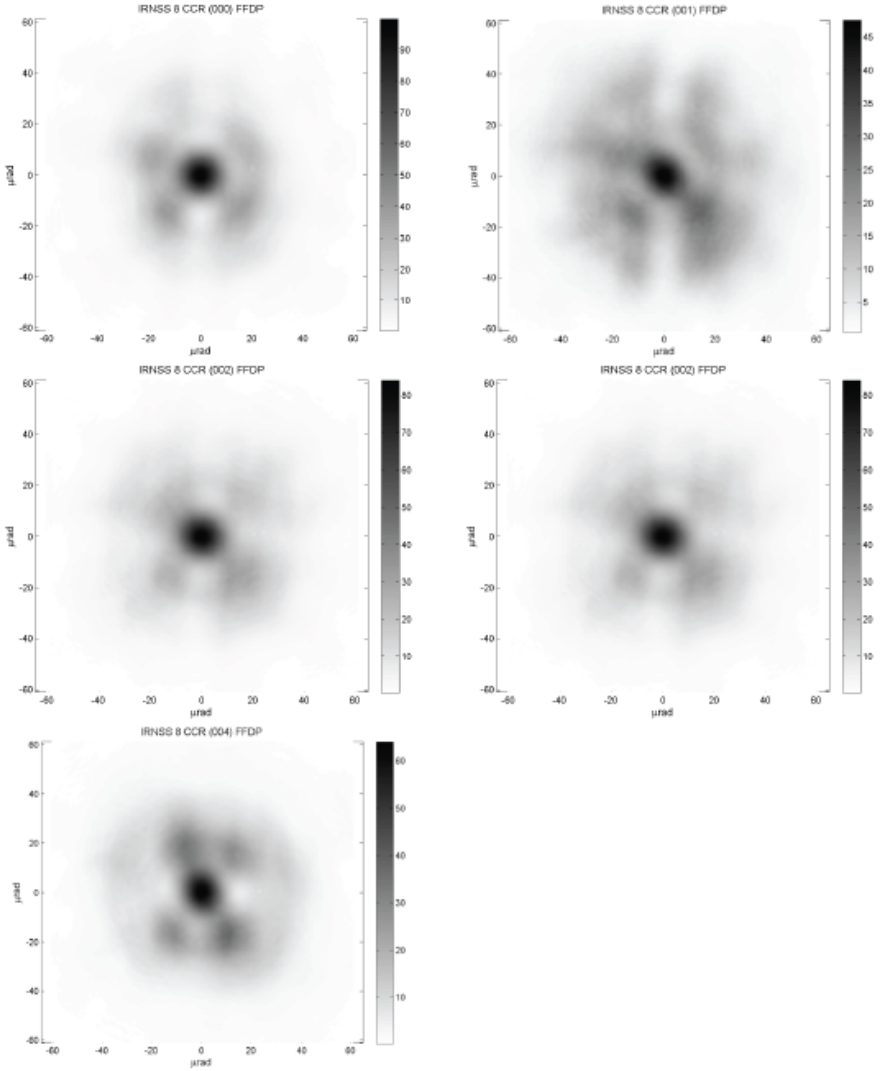

Figure 71 Sum FFDPs during IRNSS orbit test

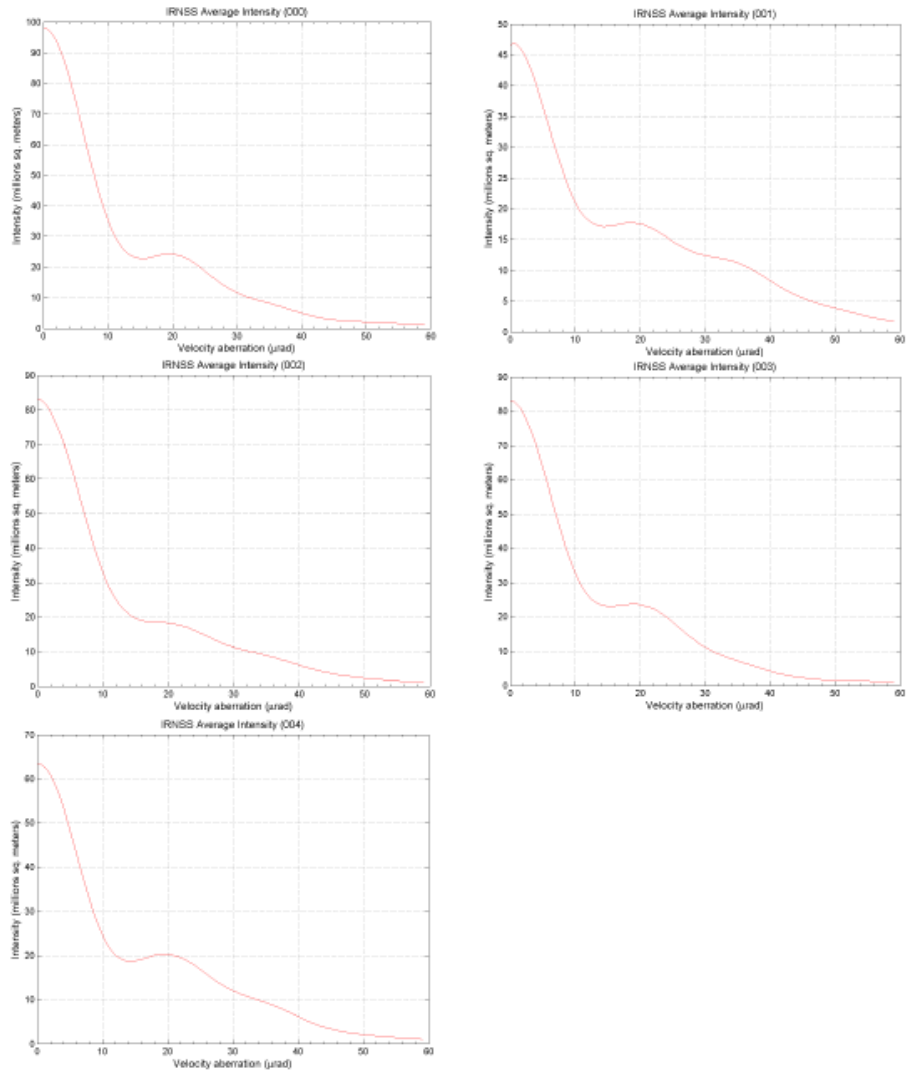

Figure 72 Sum FFDP intensity vs velocity aberration during IRNSS orbit Test

LRA SCF-Test n.2: Sun Simulator at varying angles - optical analysis for all 8 CCRs

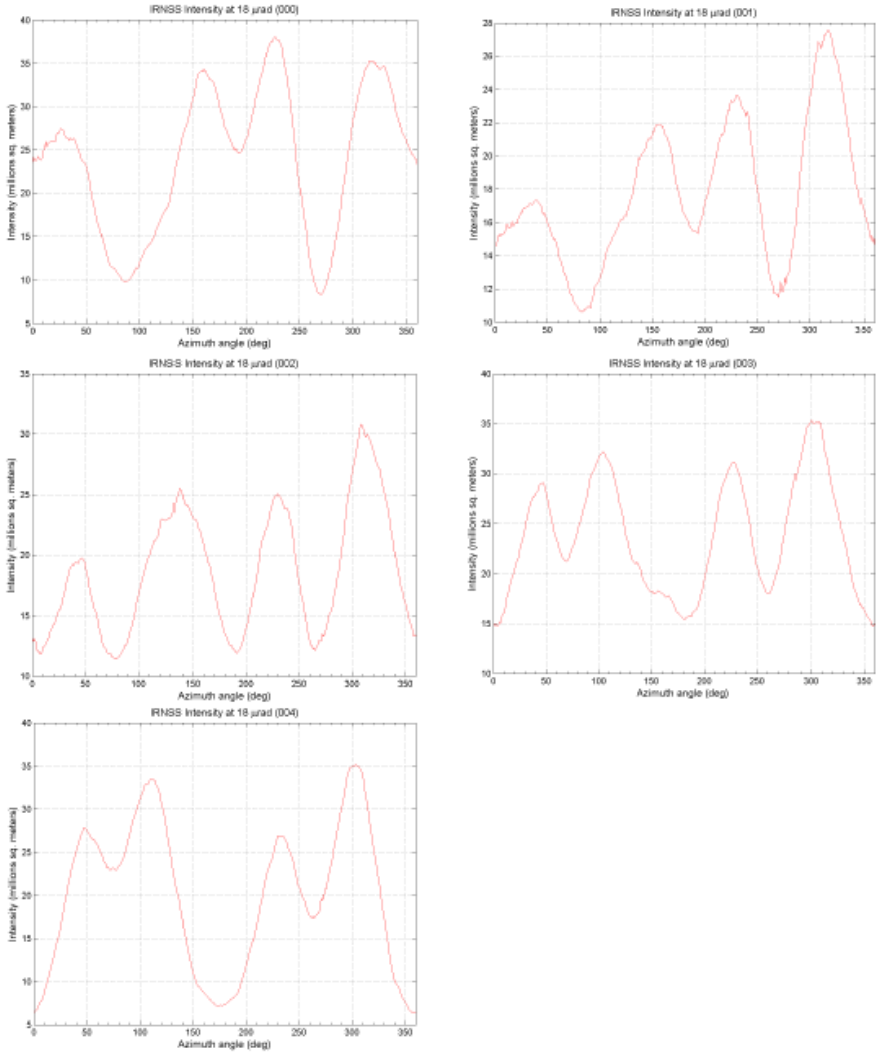

Figure 73 Sum FFDP intensity at 18µrad annulus during IRNSS orbit test

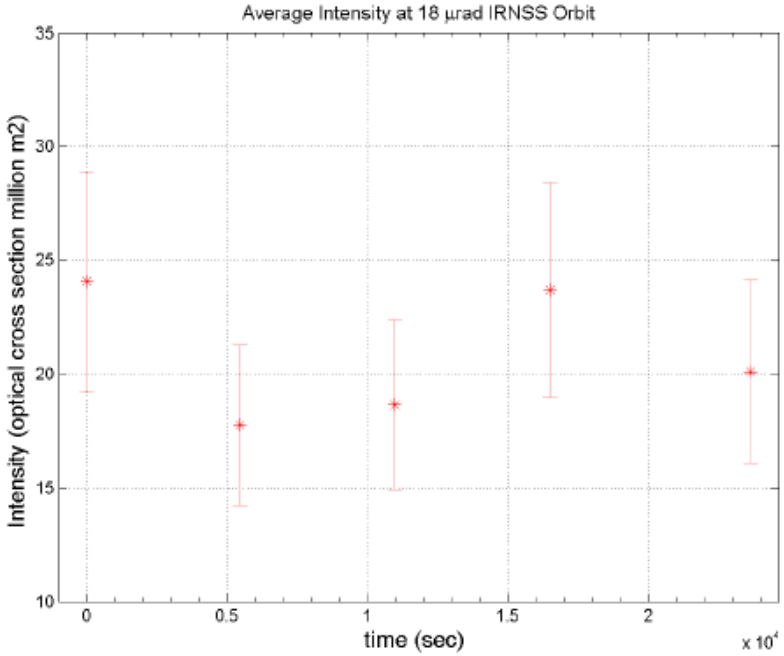

Figure 74 Average intensity variation of summed tested CCRRs at 18 µrad during orbit. Error on intensity is 20% of the relative intensity

The initial conditions (average intensity 24.03E06 m^2) are similar to the in-air and isothermal conditions (average intensity 22.97E06 m^2), calculated from Table 4 in [AD-3].

LRA SCF-Test n.3: Sun Simulator at varying angles

Test Structure:

- Sun Simulator illuminating the array **with cover installed** at changing angles, exploiting the rotation system of the SCF, with a rate of about 15˚/hour.
- Waited until the payload and the surrounding environment reached the starting equilibrium conditions (cold/vacuum and LRA tray at Ti=20˚C).
- Start with an automatic procedure which lasted 6 hours.
- FFDPs and IR pictures of each measured CCRR (x5).
- Extra valuable data and deliverables (not foreseen by [AD-1]) in order to better understand the optical and thermal behaviour of the array:
  1. Two FFDPs more than what planned in [AD-1] (one FFDP at the beginning and one at the end of the orbit).
  2. Thermal analysis based on IR pictures taken together with FFDPs.

Optical Analysis:

- Analysis of raw optical measured data with a dedicated MATLAB program.
- For each tested CCRR and laser incidence angle the program computes:
  - The Field Diffraction Pattern (FFDP) in Optical Cross Section (OCS) unit.
  - OCS intensity distribution versus velocity aberration.
  - OCS intensity distribution in annulus at 18 µrad velocity aberration.
  - Average OCS intensity at 18 µrad velocity aberration a total CCRR FFDP.

LRA SCF-Test n.3: Sun Simulator at varying angles - optical analysis

Same tests and analyses as per SCF-Test n.2 for each of the CCRs n. 8, 9, 12, 13, 21, 22, 28, 29.

LRA SCF-Test n.3: Sun Simulator at varying angles - optical analysis for all 8 CCRs

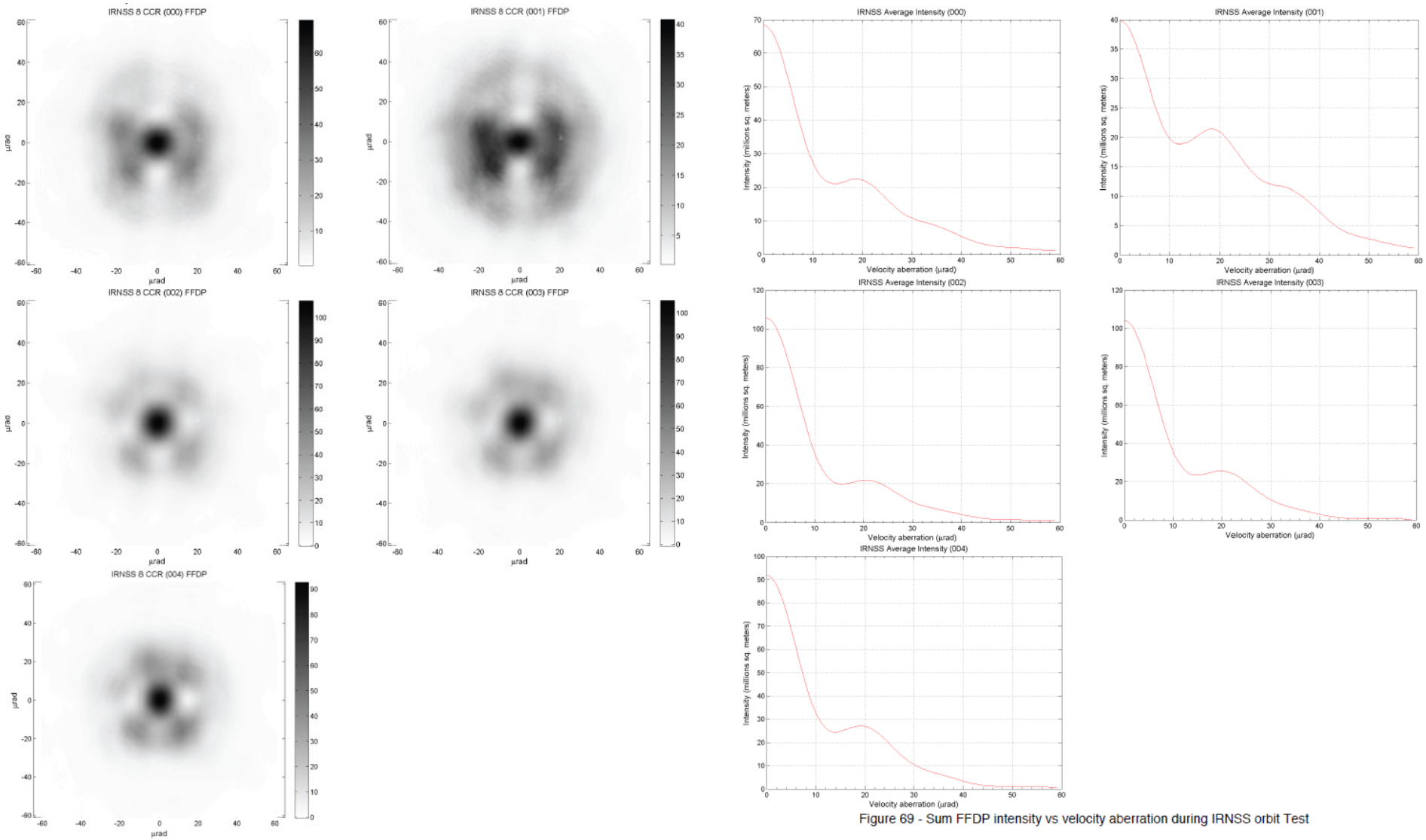

Figure 69 - Sum FFDP intensity vs velocity aberration during IRNSS orbit Test

LRA SCF-Test n.3: Sun Simulator at varying angles - optical analysis for all 8 CCRs

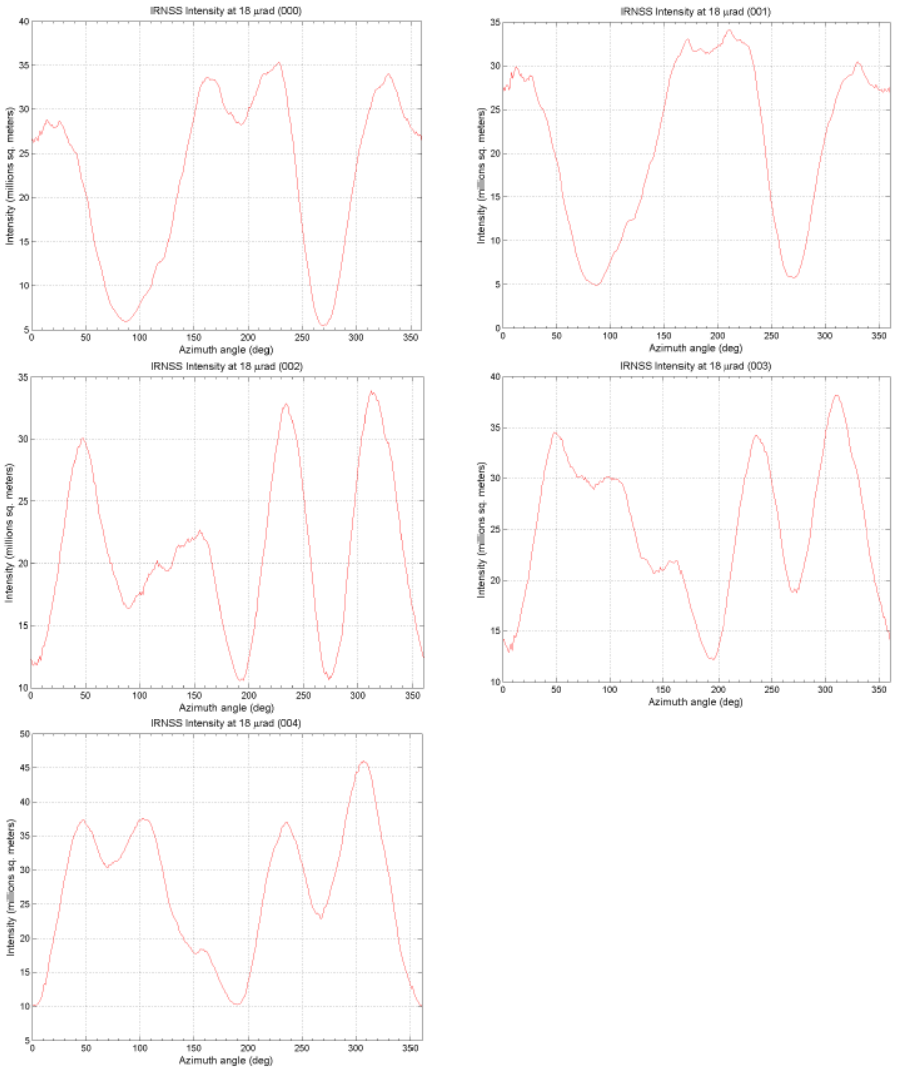

Figure 70 - Sum FFDP intensity at 18µrad annulus during IRNSS orbit test.

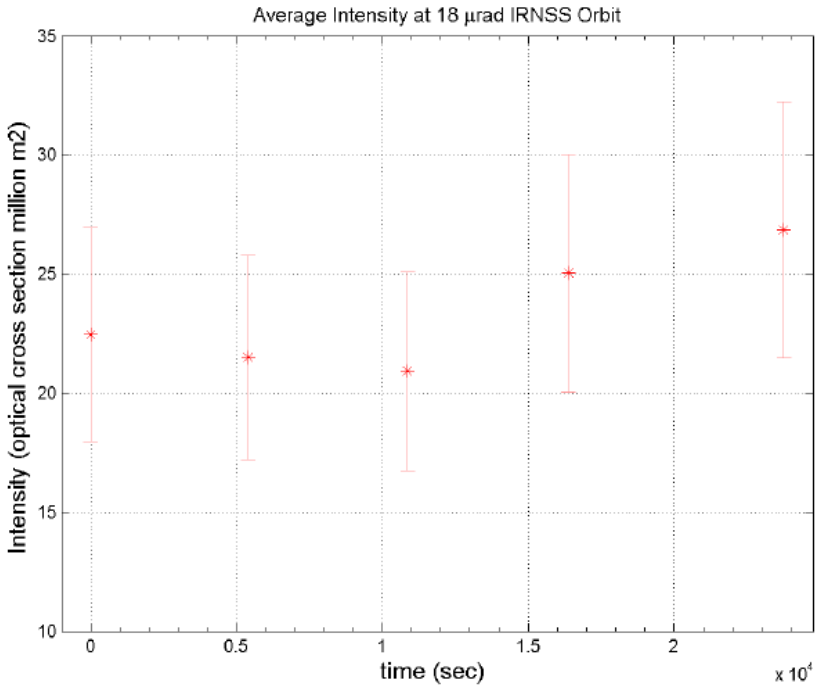

ıre 71 - Average intensity variation of summed tested CCRRs at 18 µrad during orbit. Error on intensity is 20% of the relative intensity.

ɛ initial conditions (average intensity 22.46E06 m^2) are similar to the in-air and hermal conditions (average intensity 22.97E06 m^2), calculated from Table 4 in [AD-3].

LRA SCF-Tests n.2 and n.3: Sun Simulator at varying angles - comparison

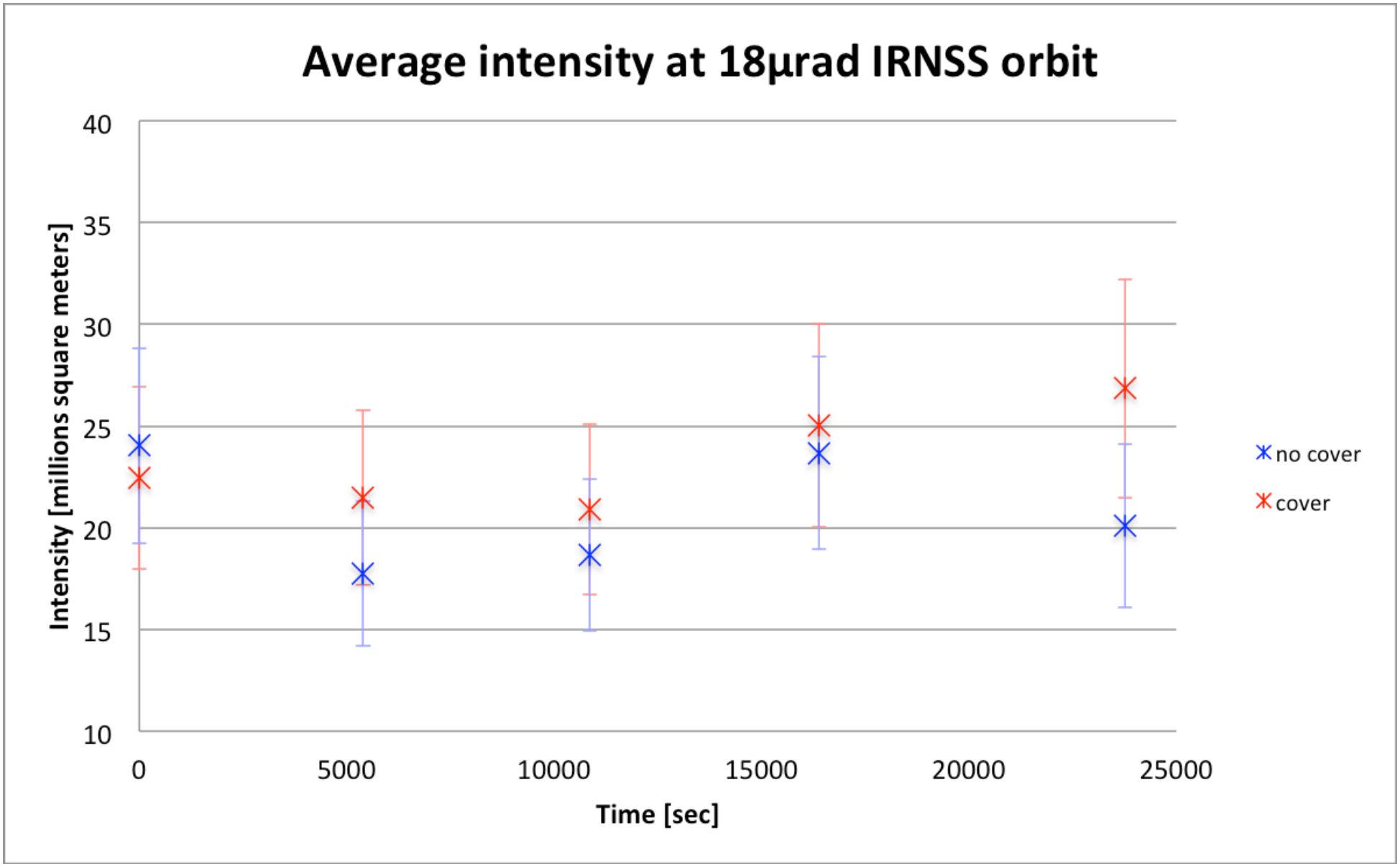

IRNSS comparison with GRA

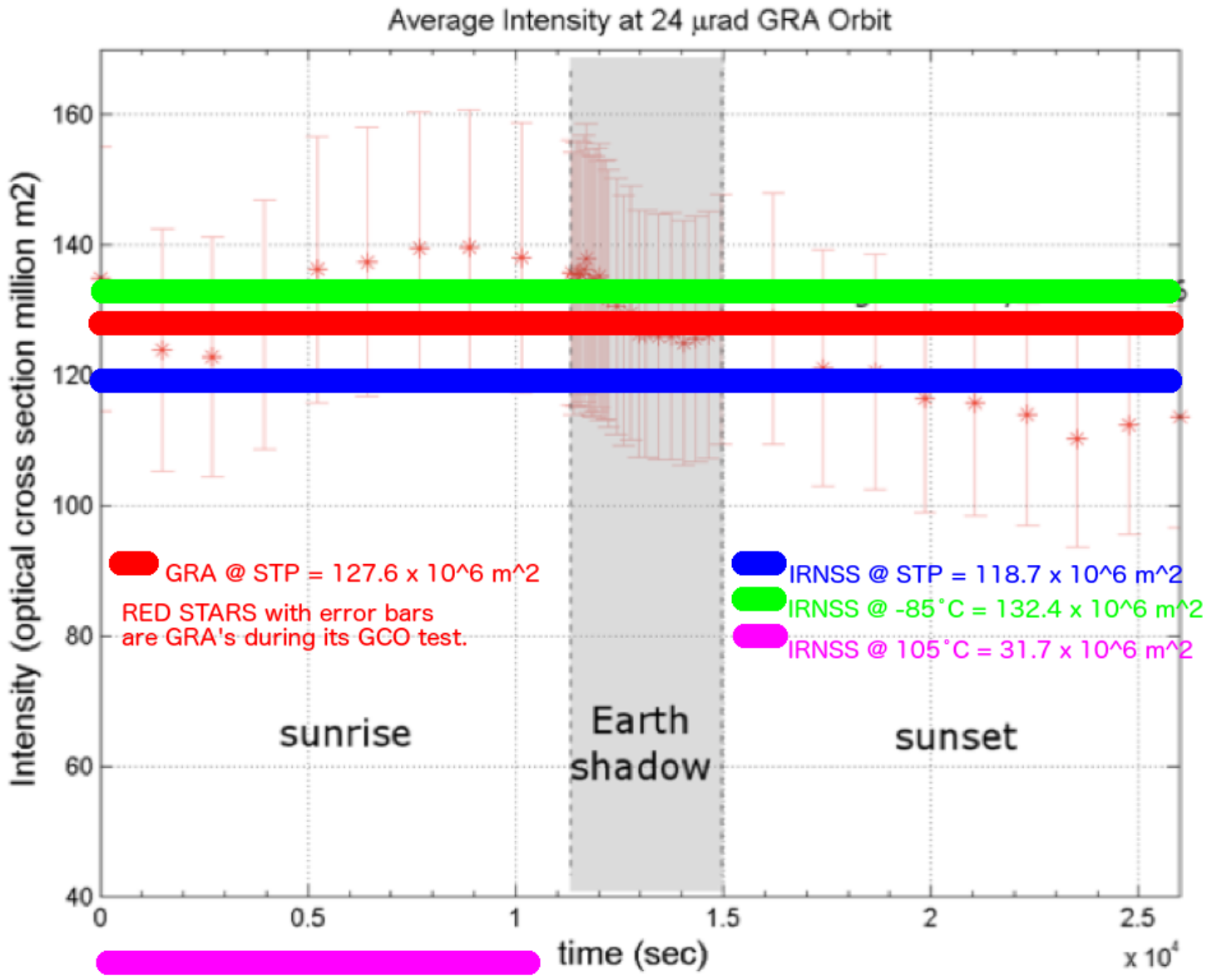

LRA SCF-Test n.2: Sun Simulator at varying angles - thermal analysis

There is a characteristic triangular temperature distribution with three hot spots corresponding to the positions where the CCRR is connected to the supporting structure.

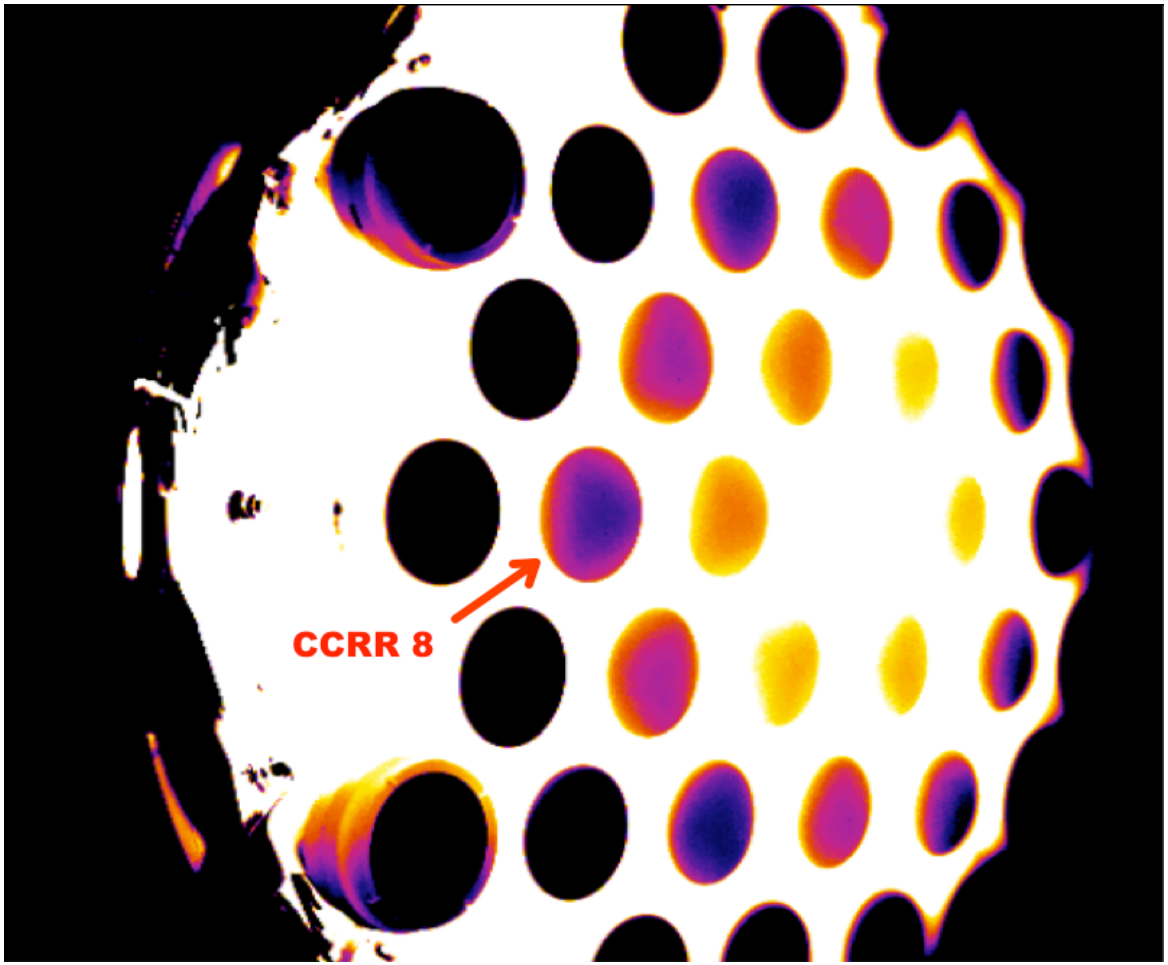

Thanks!